

## BACHELOR

### Numerical models of light scattering in a dusty plasma

Bertens, M.W.M.C.

*Award date:*  
2016

[Link to publication](#)

#### **Disclaimer**

This document contains a student thesis (bachelor's or master's), as authored by a student at Eindhoven University of Technology. Student theses are made available in the TU/e repository upon obtaining the required degree. The grade received is not published on the document as presented in the repository. The required complexity or quality of research of student theses may vary by program, and the required minimum study period may vary in duration.

#### **General rights**

Copyright and moral rights for the publications made accessible in the public portal are retained by the authors and/or other copyright owners and it is a condition of accessing publications that users recognise and abide by the legal requirements associated with these rights.

- Users may download and print one copy of any publication from the public portal for the purpose of private study or research.
- You may not further distribute the material or use it for any profit-making activity or commercial gain

# Numerical Models of Light Scattering in a Dusty Plasma

AUTHOR: M.W.M.C. BERTENS  
TECHNICAL UNIVERSITY EINDHOVEN  
ELEMENTARY PROCESSES IN GAS DISCHARGES (EPG)

SUPERVISORS:  
PROF. DR. IR. W.L. IJZERMAN  
DR. IR. J. BECKERS  
IR. L.P.T. SCHEPERS

JULY 8, 2015



## Abstract

In this thesis, simulations and derivations of the theory of light propagation in a scattering medium are presented. When light scatters at a spherical particle, it produces a characteristic pattern which is known as a Mie pattern which depends on the particle size and the wavelength of the light. The general shape of this pattern is a sine which has some high frequency oscillations. This pattern can be explained by the Mie theory, which is derived by solving the Maxwell equations. Light which scatters more than once will most likely not show a Mie pattern. To understand this, multiple models have been made which have been programmed in Matlab. In order to make this model, theory of light propagation has been derived. The results of the model show that light which scatters multiple times, remains the general shape of Mie scattering. However, the high frequency oscillations, which are characteristic for Mie pattern, disappear. This is because the oscillations of different times of scattering add and average each other out. From the model it also becomes visible that the oscillations of the pattern disappear with fewer scattering when the scattering coefficients at particles increases.

When programming a model, non-trivial mathematical results are often used. One example is numerical integration. In order to understand the mechanism, a numerical integration method is derived. This method is called the Simpson's Rule and has been extended to work for arbitrary dimensions. Furthermore, the integration error has been analyzed. As function of the discretization steps, the error of the method on a logarithmic plot is a straight line with a slope of four. Thus by doubling the amount of discretization steps, the method becomes more precise by a factor 16 which is in accordance with the theory.

## Abstract for Laymen

In this report, simulations and derivations of the theory of the behaviour of light are presented. The field of interest is the spreading of light when it hits small particles. When light hits a round particle, it produces a distinctive pattern which is known as a Mie pattern. This pattern is visualized as a big wave with a lot of small vibrations and is derived by the fundamental properties of light known as the Maxwell equations. This derivation is called the Mie theory. The Mie pattern is one big wave with many smaller waves which are vibrations. It often happens that light hits multiple particles after each other. Therefore the pattern of the measured light will not be as the Mie theory tells. To understand this, multiple models and simulations have been made which have been programmed on a computer. In order to make these simulations, the spreading of light has been studied. The results show that light which hits multiple particles, becomes more smooth; there are fewer vibrations which are distinctive for the Mie patterns. These vibrations disappear because there are highs and lows in the vibrations which cancel each other out when there are many at the same spot. It also becomes visible that the vibrations of the pattern disappear faster when the particles spread the light better.

When making a simulation, a lot of mathematics is used. One example is the calculation of surfaces. To avoid misusing the mathematics, surface calculation models have been made for a computer to use. The made method is called the Simpson's Rule. Because the computer calculates the surface, there are always some errors. These errors have been analyzed. It became clear that when there are twice as much points used, the method becomes more precise by a factor 16 which is in accordance with the theory.

# Contents

<b>1</b>	<b>Introduction</b>	<b>1</b>
<b>2</b>	<b>Theory</b>	<b>2</b>
2.1	Electromagnetic scattering . . . . .	2
2.2	Mie Theory . . . . .	5
2.2.1	Solutions to the Maxwell Equations . . . . .	6
2.2.2	Expansion of the electromagnetic fields in spherical harmonics . . . . .	10
2.2.3	Scatter Coefficients . . . . .	12
2.2.4	Mie Theory in Relation to the Scattering Matrix . . . . .	13
2.3	Light Propagation . . . . .	14
2.3.1	Differential Equation for Light Propagation . . . . .	14
2.3.2	Diffuse Light Intensity . . . . .	16
2.3.3	Integral Equation for the Diffuse Intensity . . . . .	16
2.3.4	Order Approach for the Diffuse Intensity . . . . .	18
<b>3</b>	<b>Numerical Integration</b>	<b>20</b>
3.1	Interpolation . . . . .	20
3.2	Lagrange interpolation . . . . .	21
3.3	Newton-Cotes formula . . . . .	22
3.4	Simpson's Rule . . . . .	23
3.5	Application of the Simpson's Rule . . . . .	24
<b>4</b>	<b>Models</b>	<b>26</b>
4.1	Plane Wave Incident on a Plane-Parallel Medium . . . . .	26
4.2	Plane Wave Incident on a Plane-Parallel Medium with a Finite Laser . . . . .	30
4.3	Plane Wave Incident on a Circular Medium with a Flat Laser . . . . .	33
4.4	Improvements of the Plane Wave Incident on a Circular Medium with a Flat Laser . . . . .	41
<b>5</b>	<b>Conclusion and Further Research</b>	<b>42</b>
<b>A</b>	<b>Changing the Order of Integration and Summation</b>	<b>43</b>
<b>B</b>	<b>Matlab Scripts for Simpson's Rule</b>	<b>45</b>
<b>C</b>	<b>Matlab Models</b>	<b>48</b>
C.1	Plane wave incident on a Plane-Parallel Medium . . . . .	48
C.2	Plane wave incident on a Plane-Parallel Medium with a Flat Laser . . . . .	50
C.3	Plane wave incident on a Circular Medium with a Flat Laser . . . . .	52
<b>D</b>	<b>Matlab Mie Theory</b>	<b>57</b>
	<b>References</b>	<b>61</b>



# 1 Introduction

Optics is one of the oldest branches in physics and has been studied extensively. Still, not every aspect of light is fully understood. This opens up opportunities for physicists. For example, in 2014 the nobel prize was awarded for a contribution in the field of optics. "The Nobel Prize in Physics 2014 was awarded jointly to Isamu Akasaki, Hiroshi Amano and Shuji Nakamura "for the invention of efficient blue light-emitting diodes which has enabled bright and energy-saving white light sources".<sup>[1]</sup> It is this invention which inspired this thesis. A research by ir. L.P.T. Schepers is currently conducted. For this research a plasma, which contains dust particles and which is illuminated by a laser, is analysed. The dust particles typically have a radius of 5 nanometer. That research is conducted to further improve the quality of white LED's. To mimic scatter peaks in LED applications, the main goal of this thesis will be to model such a 'dusty plasma' which is illuminated by a laser so that the experimental results can be compared to the theoretical predictions.

This thesis will start by deriving some properties of light. It starts with general light/-electromagnetic scattering. After this the scattering of light at spherical particles is analysed. The theory which explains this is called the Mie Theory<sup>[2]</sup>. This theory strongly depends on the radius and reflective index of particles and the used wave length. When the scattering is known, the propagation of light in a medium can be derived following the work of Ishimaru<sup>[3]</sup>.

In order to make a model for light propagation, numerical analysis is needed. Therefore a numerical integration method will be mathematically derived. This method uses a result known as the Newton-Cotes<sup>[4]</sup> formula. This integration method is implemented in Matlab and extended to be able to integrate over arbitrary dimensions.

At last, three models will be presented which have been programmed in Matlab. The first two can be used to model light penetrating the ocean. The last model is used to model a dusty plasma. These models will be analysed and reflected upon.



## 2 Theory

### 2.1 Electromagnetic scattering

In order to construct a theory for light scattering in a dusty plasma, some definitions have to be made. Consider a particle in a medium with dielectric constant  $\epsilon_0$  and permeability  $\mu_0$  which is illuminated by a linearly polarized electromagnetic plane wave. The normalized electric field is given by:

$$\mathbf{E}_i(\mathbf{r}) = \mathbf{e}_i \exp(ik \mathbf{s} \cdot \mathbf{r}). \quad (1)$$

Here  $i$  is the imaginary number,  $k = \omega\sqrt{\mu_0\epsilon_0} = \omega/c = 2\pi v/c = 2\pi/\lambda$  is the wave number,  $\omega$  the frequency,  $c$  the speed of light in a vacuum,  $\mathbf{r}$  the position and  $\lambda$  the wavelength. Both  $\mathbf{s}$  and  $\mathbf{e}_i$  are unit vectors with  $\mathbf{i}$  pointing in the direction of wave propagation and  $\mathbf{e}_i$  in the direction of the polarization.

When light is scattered on a particle and assumed to be a point source, the following equation holds<sup>[5]</sup>:

$$\begin{pmatrix} E_{\parallel} \\ E_{\perp} \end{pmatrix}_s = \frac{e^{ikr}}{r} \begin{pmatrix} S_1 & S_2 \\ S_3 & S_4 \end{pmatrix} \begin{pmatrix} E_{\parallel} \\ E_{\perp} \end{pmatrix}_i \quad (2)$$

Where  $E_{\parallel}$  and  $E_{\perp}$  represent the parallel and perpendicular components of the electrical field in the plane of scattering respectively. The subscripts  $s$  and  $i$  denote the scattered and incident waves respectively. The direction of propagation of the scattered wave will be denoted by the vector  $\mathbf{s}$ . Furthermore,  $r$  is the distance from the point of scattering. The matrix  $\underline{\underline{S}} = \begin{pmatrix} S_1 & S_2 \\ S_3 & S_4 \end{pmatrix}$  is known as the scattering matrix where all  $S_i$ 's can be complex and contain the amplitude and phase shift of the incident wave.

In the ideal case, where the particles are perfect spheres, the scattering components  $S_2$  and  $S_3$  are zero. This is due to the rotation invariance of spheres. When light is polarized perpendicular to the plane of incidence, it can only produce scattered light perpendicular to the plane of refraction. Therefore  $S_2$  is zero. The same argument holds for light which is only polarized parallel to the plane of incidence. Therefore  $S_3$  is zero. For a linearly polarized electromagnetic wave polarized perpendicularly to the plane of scattering the following holds:

$$\begin{aligned} \begin{pmatrix} E_{\parallel} \\ E_{\perp} \end{pmatrix}_s &= \frac{e^{ikr}}{r} \begin{pmatrix} S_1 & 0 \\ 0 & S_4 \end{pmatrix} \begin{pmatrix} 0 \\ E_{\perp} \end{pmatrix}_i \\ &= \frac{e^{ikr}}{r} S_4 \begin{pmatrix} 0 \\ E_{\perp} \end{pmatrix}_i \end{aligned} \quad (3)$$

So we can conclude that light which is polarized perpendicular to the scattering plane will still be linearly polarized after scattering on an ideal particle. A similar result holds

for polarized light parallel to the scatter plane.

It is often desired to capture a concept in a general manner. This is also the case for light scattering. Therefor consider polarized light with unknown polarization incident on a non ideal particle. From equation 2 it follows

$$\begin{aligned} E_{\parallel,s} &= \frac{e^{ikr}}{r}(S_1 E_{\parallel,i} + S_2 E_{\perp,i}) \\ E_{\perp,s} &= \frac{e^{ikr}}{r}(S_3 E_{\parallel,i} + S_4 E_{\perp,i}) \end{aligned} \quad (4)$$

which are the componentwise equations of equation 2. The light intensity is given by  $I = \frac{\epsilon_0 c n}{2} |\mathbf{E}|^2$  for monochromatic waves, where  $c$  is the speed of light in a vacuum and  $n$  the refraction index of the medium. Because we are considering plane waves, which are monochromatic waves, it is sufficient to state  $I \sim |\mathbf{E}|^2$ . For non-monochromatic waves the magnitude of the pointing-vector should be used to derive the light intensity. From the first equation of 4 follows:

$$\begin{aligned} |E_{\parallel,s}|^2 &= \frac{1}{r^2} |S_1 E_{\parallel,i} + S_2 E_{\perp,i}|^2 \\ &= \frac{1}{r^2} (|S_1|^2 |E_{\parallel,i}|^2 + |S_2|^2 |E_{\perp,i}|^2 + S_1 \overline{S_2} E_{\parallel,i} \overline{E_{\perp,i}} + \overline{S_1} S_2 \overline{E_{\parallel,i}} E_{\perp,i}). \end{aligned} \quad (5)$$

From the second equation of 4 we obtain:

$$\begin{aligned} |E_{\perp,s}|^2 &= \frac{1}{r^2} |S_3 E_{\parallel,i} + S_4 E_{\perp,i}|^2 \\ &= \frac{1}{r^2} (|S_3|^2 |E_{\parallel,i}|^2 + |S_4|^2 |E_{\perp,i}|^2 + S_3 \overline{S_4} E_{\parallel,i} \overline{E_{\perp,i}} + \overline{S_3} S_4 \overline{E_{\parallel,i}} E_{\perp,i}) \end{aligned} \quad (6)$$

When 5 and 6 are added to get  $|\mathbf{E}_s|^2 = |E_{\perp,s}|^2 + |E_{\parallel,s}|^2$  we obtain:

$$\begin{aligned} |E_{\parallel,s}|^2 + |E_{\perp,s}|^2 &= \frac{1}{r^2} ( (|S_1|^2 + |S_3|^2) |E_{\parallel,i}|^2 + (|S_2|^2 + |S_4|^2) |E_{\perp,i}|^2 \\ &\quad + (S_1 \overline{S_2} + S_3 \overline{S_4}) E_{\parallel,i} \overline{E_{\perp,i}} + (\overline{S_1} S_2 + \overline{S_3} S_4) \overline{E_{\parallel,i}} E_{\perp,i} ) \end{aligned} \quad (7)$$

If we assume the incident wave to be linearly polarized then either  $E_{\parallel,i} = 0$  or  $E_{\perp,i} = 0$ . Without loss of generality we assume  $E_{\perp,i} = 0$ . This reduces equation 7 to:

$$|\mathbf{E}_s|^2 = |E_{\parallel,s}|^2 + |E_{\perp,s}|^2 = \frac{1}{r^2} (|S_1|^2 + |S_3|^2) |E_{\parallel,i}|^2, \quad (8)$$

which is equal to the flux density at a distance  $r$ . The incident flux density is given by  $|\mathbf{E}_i|^2 = |E_{\parallel,i}|^2 + |E_{\perp,i}|^2 = |E_{\parallel,i}|^2$  because we assumed  $E_{\perp,i} = 0$ . We define the direction of the incident wave by the vector  $\mathbf{t}$ . The cross section of the light scattering towards  $\mathbf{s}$  from  $\mathbf{t}$  at a point, observed from the far field is called the differential scattering cross section  $\sigma_D(\mathbf{s}, \mathbf{t})$  and is given by

$$\begin{aligned}
\sigma_D(\mathbf{s}, \mathbf{t}) &= \lim_{r \rightarrow \infty} r^2 \frac{|\mathbf{E}_s|^2}{|\mathbf{E}_t|^2} \\
&= \lim_{r \rightarrow \infty} r^2 \frac{|E_{\parallel,s}|^2 + |E_{\perp,s}|^2}{|E_{\parallel,t}|^2 + |E_{\perp,t}|^2} \\
&\stackrel{(8)}{=} \lim_{r \rightarrow \infty} \frac{r^2 (|S_1|^2 + |S_3|^2) |E_{\parallel,t}|^2}{r^2 |E_{\parallel,t}|^2} \\
&= (|S_1|^2 + |S_3|^2).
\end{aligned} \tag{9}$$

When the polarization would have been in the direction of  $\mathbf{E}_{\perp,i}$  a similar result would have been obtained, namely:  $\sigma_D(\mathbf{s}, \mathbf{t}) = (|S_2|^2 + |S_4|^2)$ .

Because we do not want to limit ourselves to the method of obtaining the differential scattering cross section as discussed, we define a new function which captures this concept in a more abstract way. This is the phase function  $p(\mathbf{s}, \mathbf{t})$  which gives the coefficients for scattering, intuitively this is the fraction of light which scatters from  $\mathbf{t}$  to  $\mathbf{s}$ , so that

$$\sigma_D(\mathbf{s}, \mathbf{t}) = \frac{\sigma_t}{4\pi} p(\mathbf{s}, \mathbf{t}), \tag{10}$$

holds. where  $\sigma_t$  is given by

$$\sigma_t = \sigma_a + \sigma_s. \tag{11}$$

This is the total dissipative cross section containing the scattering cross section ( $\sigma_s$ ) and the absorption cross section ( $\sigma_a$ ). The scattering cross section equals the total scattering from all directions which is calculated by integrating over all possible incident directions  $\hat{\mathbf{s}}$  thus:

$$\sigma_s(\mathbf{t}) = \int_{4\pi} \sigma_D(\hat{\mathbf{s}}, \mathbf{t}) d\hat{\omega} = \int_{4\pi} \frac{\sigma_t}{4\pi} p(\hat{\mathbf{s}}, \mathbf{t}) d\hat{\omega}. \tag{12}$$

where  $\hat{\omega}$  is the solid angle. Thus making the scattering cross section dependant of the incident direction ( $\mathbf{t}$ ). In the next section we will assume that the scattering particles are spheres. Therefor the scattering cross section will be equal for all the incident directions. For simplicity we can therefor write  $\sigma_s(\mathbf{t})$  as  $\sigma_s$ . This latter notation will be used for the rest of this thesis.

When assuming the scattered light behaves as a point source, we could choose to define  $\mathbf{E}_s$  as

$$\mathbf{E}_s(\mathbf{r}) = \mathbf{f}(\mathbf{s}, \mathbf{t}) \frac{e^{ikr}}{r} \tag{13}$$

By using equation 2 we then obtain:

$$\mathbf{f}(\mathbf{s}, \mathbf{t}) = \begin{pmatrix} S_1 & S_2 \\ S_3 & S_4 \end{pmatrix} \begin{pmatrix} E_{\parallel} \\ E_{\perp} \end{pmatrix}_t = \begin{pmatrix} S_1 \cdot E_{\parallel,t} + S_2 \cdot E_{\perp,t} \\ S_3 \cdot E_{\parallel,t} + S_4 \cdot E_{\perp,t} \end{pmatrix} \quad (14)$$

This implies

$$\begin{aligned} \sigma_D(\mathbf{s}, \mathbf{t}) &= \lim_{r \rightarrow \infty} r^2 \frac{|\mathbf{E}_s|^2}{|\mathbf{E}_t|^2} \\ &= \lim_{r \rightarrow \infty} \frac{r^2}{r^2} \frac{|\mathbf{f}(\mathbf{s}, \mathbf{t})|^2}{|\mathbf{E}_t|^2} \\ &= |\mathbf{f}(\mathbf{s}, \mathbf{t})|^2. \end{aligned} \quad (15)$$

The last step in equation 15 holds because we assumed the incident wave to be normalised. We thus can conclude that

$$\sigma_D(\mathbf{s}, \mathbf{t}) = |\mathbf{f}(\mathbf{s}, \mathbf{t})|^2 = \frac{\sigma_t}{4\pi} p(\mathbf{s}, \mathbf{t}) \quad (16)$$

and

$$\sigma_s(\mathbf{t}) = \int_{4\pi} \sigma_d(\hat{\mathbf{s}}, \mathbf{t}) d\hat{\omega} = \int_{4\pi} |f(\hat{\mathbf{s}}, \mathbf{t})|^2 d\hat{\omega} = \int_{4\pi} \frac{\sigma_t}{4\pi} p(\hat{\mathbf{s}}, \mathbf{t}) d\hat{\omega}. \quad (17)$$

holds. This way it is also possible to derive the differential scattering cross section in other manners such as by using Maxwell's equation. One of the results from Maxwell's equations is the Mie Theory which provides the scattering coefficients  $S_1$  and  $S_4$  while assuming  $S_2 = S_3 = 0$ . This will be discussed in the next section. With these results we can rewrite equation 14 as

$$\mathbf{f}(\mathbf{s}, \mathbf{t}) = \begin{pmatrix} S_1 \cdot E_{\parallel,t} \\ S_4 \cdot E_{\perp,t} \end{pmatrix} \quad (18)$$

thus  $|\mathbf{f}(\mathbf{s}, \mathbf{t})|^2 = |S_1 \cdot E_{\parallel,t}|^2 + |S_4 \cdot E_{\perp,t}|^2 = \sigma_D(\mathbf{s}, \mathbf{t}) = \frac{\sigma_t}{4\pi} p(\mathbf{s}, \mathbf{t})$ .

## 2.2 Mie Theory

For light scattering on spherical particles it is possible to calculate the scattering coefficients analytically. This can be done by Mie Theory. Mie Theory solves the associated Maxwell equations by constructing functions with properties which satisfy the Maxwell equations. In the next section we will derive the solutions to the Maxwell equations. For the derivation of Mie theory, privately shared work of Schepers<sup>[6]</sup> was used. For a more formal and complete derivation we refer to Bohren and Huffman<sup>[2]</sup>.

### 2.2.1 Solutions to the Maxwell Equations

To derive the Mie theory, we start with constructing two fields  $\mathbf{M}$  and  $\mathbf{N}$  which satisfy the Maxwell equations. When light is considered as a wave, the electrical and magnetic portions oscillate in time and so can be written as

$$\begin{aligned}\nabla \times \mathbf{E}(\mathbf{x}, t) &= E(\mathbf{x})e^{-i\omega t} \\ \nabla \times \mathbf{H}(\mathbf{x}, t) &= H(\mathbf{x})e^{-i\omega t}\end{aligned}\tag{19}$$

where  $\mathbf{E}$  and  $\mathbf{H}$  are the electric and magnetic field respectively. Furthermore,  $x$  is the position,  $t$  is the time and  $\omega$  is the oscillation frequency. This reduces the Maxwell equations to

$$\nabla \cdot \mathbf{E}(\mathbf{x}) = 0\tag{20}$$

$$\nabla \cdot \mathbf{H}(\mathbf{x}) = 0\tag{21}$$

$$\nabla \times \mathbf{E}(\mathbf{x}) = -i\omega\mu\mathbf{H}(\mathbf{x})\tag{22}$$

$$\nabla \times \mathbf{H}(\mathbf{x}) = i\omega\epsilon\mathbf{E}(\mathbf{x})\tag{23}$$

$$(24)$$

where  $\mu$  and  $\epsilon$  are the electric and magnetic permeability respectively. From the wave equations

$$\begin{aligned}\nabla^2\mathbf{E}(\mathbf{x}) + k^2\mathbf{E}(\mathbf{x}) &= 0 \\ \nabla^2\mathbf{H}(\mathbf{x}) + k^2\mathbf{H}(\mathbf{x}) &= 0\end{aligned}\tag{25}$$

can be derived where  $k = \omega^2\epsilon\mu$ . Because we are dealing with spherical particles it is convenient to solve these equations in spherical coordinates. To do so we will construct the vectors  $\mathbf{M}$  and  $\mathbf{N}$  in such that they obey equations 20 - 23 and 25. These equations state that  $\mathbf{M}$  and  $\mathbf{N}$  are:

1. divergence free (equations 20 and 21),
2. and satisfying the wave equations (equations 25).
3. the curl of one, is proportional to the other (equations 22 and 23),

We assume

$$\mathbf{M} = \nabla \times (\mathbf{r}\psi)\tag{26}$$

where  $\psi$  is a scalar field and  $\mathbf{r}$  is the radius vector with its origin in the center of the scattering particle (sphere). By defining  $\mathbf{M}$  in this way,  $\mathbf{M}$  satisfies the first criterium automatically. By taking twice the curl on both sides of equation 26 and using the vector relations

$$\nabla \times \nabla \times \nabla \times \mathbf{A} = -\nabla \times (\nabla^2 \mathbf{A}) \quad (27)$$

$$\nabla(\nabla \cdot \mathbf{A}) - \nabla \times \nabla \times \mathbf{A} = \nabla^2 \mathbf{A} \quad (28)$$

we obtain

$$\nabla^2 \mathbf{M} + k^2 \mathbf{M} = \nabla \times [\mathbf{r}(\nabla^2 \psi + k^2 \psi)] \quad (29)$$

Thus  $\mathbf{M}$  satisfies the wave equation when  $\psi$  satisfies the scalar equation

$$\nabla^2 \psi + k^2 \psi = 0. \quad (30)$$

Then  $\mathbf{M}$  also satisfies the second equation. Defining the second vector  $\mathbf{N}$  by

$$\mathbf{N} = \frac{\nabla \times \mathbf{M}}{k}, \quad (31)$$

implies

$$\nabla \times \mathbf{N} = k \mathbf{M} \quad (32)$$

should hold in order for  $\mathbf{N}$  to satisfy the wave equation. By this definition of  $\mathbf{N}$  the third criterium is also met, because applying equation 28 to equations 31 and 32 implies  $\nabla^2 \mathbf{N} + k^2 \mathbf{N} = 0$ . This implies that  $\mathbf{M}$  and  $\mathbf{N}$  can be used to construct the electric and magnetic fields when  $\psi$  is found by solving the scalar wave equation. The scalar wave equation in spherical coordinates is given by

$$\frac{1}{r^2} \frac{\partial}{\partial r} \left( r^2 \frac{\partial \psi}{\partial r} \right) + \frac{1}{r^2 \sin \theta} \frac{\partial}{\partial \theta} \left( \sin \theta \frac{\partial \psi}{\partial \theta} \right) + \frac{1}{r^2 \sin \theta} \frac{\partial^2 \psi}{\partial \phi^2} + k^2 \psi = 0. \quad (33)$$

This differential equation can be solved by using the method of separation of variables. The solution is given in the form of

$$\psi(r, \theta, \phi) = R(r)\Theta(\theta)\Phi(\phi) \quad (34)$$

where  $R$ ,  $\Theta$  and  $\Phi$  are functions of the common spherical coordinates  $r$ ,  $\theta$  and  $\phi$ . This solution reduces the differential equation 33 to three separated differential equations which are given by

$$\frac{d^2\Phi}{d\psi^2} + m^2 = 0 \quad (35)$$

$$\frac{1}{\sin\theta} \frac{d}{d\theta} \left( \sin\theta \frac{\partial\Theta}{\partial\theta} \right) + \left( n(n+1) - \frac{m^2}{\sin^2\theta} \right) \Theta = 0 \quad (36)$$

$$\frac{d}{dr} \left( r^2 \frac{dR}{dr} \right) + (k^2 r^2 - n(n+1)) R = 0 \quad (37)$$

where  $m$  and  $n$  are separation constants. Equation 35 has two linearly independent solutions:

$$\Phi_e = \cos(m\phi), \quad (38)$$

$$\Phi_o = \sin(m\phi). \quad (39)$$

The subscripts  $e$  and  $o$  denote the even and odd solutions respectively. Because  $\Phi(\phi)$  is periodic with  $2\pi$ ,  $m$  should be an integer so that  $\Phi(\phi) = \Phi(\phi + 2\pi)$ . Because the solutions  $\Phi_e$  and  $\Phi_o$  are linearly independent,  $m$  should also be non-negative because for negative  $m$  the solutions can be dependent. The solution of 36 is given by

$$\Theta = P_n^m(\cos\theta) \quad (40)$$

where  $P_n^m$  are Legendre polynomials of degree  $n = m, m+1, \dots$  and order  $m$ . The solutions to equation 37 are given by the spherical Bessel function  $z_n(kr)$  of order  $n$  which can be of the first or second kind. These are given by

$$j_n(kr) = \sqrt{\frac{\pi}{2kr}} J_{n+1/2}(kr) \quad (41)$$

$$y_n(kr) = \sqrt{\frac{\pi}{2kr}} Y_{n+1/2}(kr) \quad (42)$$

with  $J_{n+1/2}(kr)$  and  $Y_{n+1/2}(kr)$  normal Bessel functions of order  $n + \frac{1}{2}$  of the first and second kind respectively. Linearly independent combinations of these two spherical Bessel functions are also solutions to the differential equation 37. These so called Hankel functions are given by

$$h_n^{(1)}(kr) = j_n(kr) + iy_n(kr) \quad (43)$$

$$h_n^{(2)}(kr) = j_n(kr) - iy_n(kr) \quad (44)$$

With these solutions of 35, 36 and 37, the solutions for  $\psi$  to the scalar wave equation are given by

$$\psi_{emn} = \cos(m\phi)P_n^m(\cos\theta)z_n(kr) \quad (45)$$

$$\psi_{omn} = \sin(m\phi)P_n^m(\cos\theta)z_n(kr) \quad (46)$$

which are used to construct the general solutions of  $\mathbf{M}$  and  $\mathbf{N}$ . These are given by

$$\begin{aligned} \mathbf{M}_{emn} &= -\frac{m}{\sin\theta} \sin(m\phi)P_n^m(\cos\theta)z_n(kr)\hat{\mathbf{e}}_\theta \\ &\quad - \cos(m\phi)\frac{dP_n^m(\cos\theta)}{d\theta}z_n(kr)\hat{\mathbf{e}}_\phi \end{aligned} \quad (47)$$

$$\begin{aligned} \mathbf{M}_{omn} &= \frac{m}{\sin\theta} \sin(m\phi)P_n^m(\cos\theta)z_n(kr)\hat{\mathbf{e}}_\theta \\ &\quad - \sin(m\phi)\frac{dP_n^m(\cos\theta)}{d\theta}z_n(kr)\hat{\mathbf{e}}_\phi \end{aligned} \quad (48)$$

$$\begin{aligned} \mathbf{N}_{emn} &= -\frac{z_n(kr)}{kr} \cos(m\phi)n(n+1)P_n^m(\cos\theta)\hat{\mathbf{e}}_r \\ &\quad + \cos(m\phi)\frac{dP_n^m(\cos\theta)}{d\theta}\frac{1}{kr}\frac{d}{dkr}(krz_n(kr))\hat{\mathbf{e}}_\theta \\ &\quad - m\sin(m\phi)\frac{dP_n^m(\cos\theta)}{\sin\theta}\frac{1}{kr}\frac{d}{dkr}(krz_n(kr))\hat{\mathbf{e}}_\phi \end{aligned} \quad (49)$$

$$\begin{aligned} \mathbf{N}_{omn} &= \frac{z_n(kr)}{kr} \sin(m\phi)n(n+1)P_n^m(\cos\theta)\hat{\mathbf{e}}_r \\ &\quad + \sin(m\phi)\frac{dP_n^m(\cos\theta)}{d\theta}\frac{1}{kr}\frac{d}{dkr}(krz_n(kr))\hat{\mathbf{e}}_\theta \\ &\quad + m\cos(m\phi)\frac{dP_n^m(\cos\theta)}{\sin\theta}\frac{1}{kr}\frac{d}{dkr}(krz_n(kr))\hat{\mathbf{e}}_\phi \end{aligned} \quad (50)$$

These equations are mutually orthogonal (for proof: Bohren and Huffman), and therefore it is possible to expand a plane wave in spherical harmonics. This is done in the next section by following Bohren and Huffman<sup>[2]</sup>.



### 2.2.2 Expansion of the electromagnetic fields in spherical harmonics

The electric field of an incoming plane wave, polarized in the  $x$  direction is given by

$$\mathbf{E}_i = E_0 e^{ikr \cos \theta} \mathbf{e}_x = E_0 e^{ikr \cos \theta} [\sin \theta \cos \phi \mathbf{e}_r + \cos \theta \cos \phi \mathbf{e}_\theta - \sin \phi \mathbf{e}_\phi] \quad (51)$$

where  $\mathbf{E}_i$  is the oscillating electric field incident on the sphere. The expansion of this electric field in spherical coordinates is of the form

$$\mathbf{E}_i = \sum_{m=0}^{\infty} \sum_{n=m}^{\infty} (B_{emn} \mathbf{M}_{emn} + B_{omn} \mathbf{M}_{omn} + A_{emn} \mathbf{N}_{emn} + A_{omn} \mathbf{N}_{omn}) \quad (52)$$

where  $A$  and  $B$  are the expansion coefficients which can be determined by

$$A_{emn} = \frac{\int_0^{2\pi} \int_0^\pi \mathbf{E}_i \cdot \mathbf{N}_{emn} \sin \theta \, d\theta \, d\phi}{\int_0^{2\pi} \int_0^\pi |\mathbf{N}_{emn}|^2 \sin \theta \, d\theta \, d\phi} \quad (53)$$

$$A_{omn} = \frac{\int_0^{2\pi} \int_0^\pi \mathbf{E}_i \cdot \mathbf{N}_{omn} \sin \theta \, d\theta \, d\phi}{\int_0^{2\pi} \int_0^\pi |\mathbf{N}_{omn}|^2 \sin \theta \, d\theta \, d\phi} \quad (54)$$

$$B_{emn} = \frac{\int_0^{2\pi} \int_0^\pi \mathbf{E}_i \cdot \mathbf{M}_{emn} \sin \theta \, d\theta \, d\phi}{\int_0^{2\pi} \int_0^\pi |\mathbf{M}_{emn}|^2 \sin \theta \, d\theta \, d\phi} \quad (55)$$

$$B_{omn} = \frac{\int_0^{2\pi} \int_0^\pi \mathbf{E}_i \cdot \mathbf{M}_{omn} \sin \theta \, d\theta \, d\phi}{\int_0^{2\pi} \int_0^\pi |\mathbf{M}_{omn}|^2 \sin \theta \, d\theta \, d\phi} \quad (56)$$

Because of the orthogonality between the sine and the cosine, the coefficients  $B_{emn}$  and  $A_{omn}$  vanish. Because of the orthogonality between sine and all its higher harmonics,  $A_{emn}$  and  $B_{omn}$  become 0 except for when  $m = 1$ . Because the Bessel function of the second kind has a singularity in zero, only the spherical Bessel functions of the first kind are used. This reduces the electric field to

$$\mathbf{E}_i = \sum_{n=1}^{\infty} \left( B_{o1n} \mathbf{M}_{o1n}^{(1)} + A_{e1n} \mathbf{M}_{e1n}^{(1)} \right) \quad (57)$$

where the subscript (1) is used to denote the Bessel functions of the first kind. By using equations 53 and 56, the electric field becomes

$$\mathbf{E}_i = E_0 \sum_{n=1}^{\infty} i^n \frac{2n+1}{n(n+1)} \left( \mathbf{M}_{o1n}^{(1)} - i \mathbf{N}_{e1n}^{(1)} \right). \quad (58)$$

The corresponding magnetic field follows from equations 20 - 23 and is given by

$$\mathbf{H}_i = -\frac{k}{\omega\mu} E_0 \sum_{n=1}^{\infty} i^n \frac{2n+1}{n(n+1)} \left( \mathbf{M}_{e1n}^{(1)} + i\mathbf{N}_{o1n}^{(1)} \right). \quad (59)$$

Analogue to the derivation of these incident electric and magnetic fields, the fields in the scattering sphere can be determined. The wave number and the magnetic permeability within the sphere are denoted by  $k_{int}$  and  $\mu_{int}$  respectively. Furthermore, the same arguments of orthogonality hold within the sphere. The internal fields should be finite in the origin and therefor only the Bessel functions of the first kind are used. The internal fields are given by

$$\mathbf{E}_{int} = E_0 \sum_{n=1}^{\infty} i^n \frac{2n+1}{n(n+1)} \left( c_n \mathbf{M}_{o1n}^{(1)} - i d_n \mathbf{N}_{e1n}^{(1)} \right) \quad (60)$$

$$\mathbf{H}_{int} = -\frac{k_{int}}{\omega\mu_{int}} E_0 \sum_{n=1}^{\infty} i^n \frac{2n+1}{n(n+1)} \left( d_n \mathbf{M}_{e1n}^{(1)} + i c_n \mathbf{N}_{o1n}^{(1)} \right). \quad (61)$$

$c_n$  And  $d_n$  are the expansion coefficients for the internal fields. The derivation of the scattered fields is analogue to the derivation of the incoming fields. Instead of Bessel functions, Hankel functions of the first type are used because of it's asymptotic behaviour. An approximation of these Hankel functions if given by

$$h_n^{(1)}(kr) \sim \frac{(-i)^n e^{ikr}}{ikr} \quad (62)$$

$$h_n^{(2)}(kr) \sim \frac{i^n e^{-ikr}}{ikr} \quad (63)$$

$$(64)$$

where the Hankel function of the first kind ( $h_n^{(1)}$ ) represents an outgoing wave and the Hankel function of the second kind ( $h_n^{(2)}$ ) represents an incoming wave. Therefore the expansion of the scattered wave is given by

$$\mathbf{E}_s = E_0 \sum_{n=1}^{\infty} i^n \frac{2n+1}{n(n+1)} \left( -b_n \mathbf{M}_{o1n}^{(3)} + i a_n \mathbf{N}_{e1n}^{(3)} \right) \quad (65)$$

$$\mathbf{H}_s = -\frac{k}{\omega\mu} E_0 \sum_{n=1}^{\infty} i^n \frac{2n+1}{n(n+1)} \left( a_n \mathbf{M}_{e1n}^{(3)} + i b_n \mathbf{N}_{o1n}^{(3)} \right). \quad (66)$$

### 2.2.3 Scatter Coefficients

To determine the scattered fields one must know the expansion coefficients  $a_n$  and  $b_n$ . These are often called the scatter coefficients. If we also want to solve the expansion coefficients for the internal fields ( $c_n$  and  $d_n$ ), we will need to solve for four unknowns. The solutions to these unknowns are found in the boundary conditions for the fields at the edge of the scattering sphere of radius  $a$ . These boundary conditions are given by

$$\begin{aligned}
E_{1\theta} &= E_{i\theta} + E_{s\theta} \\
E_{1\phi} &= E_{i\phi} + E_{s\phi} \\
H_{1\theta} &= H_{i\theta} + H_{s\theta} \\
H_{1\phi} &= H_{i\phi} + H_{s\phi}
\end{aligned} \tag{67}$$

where the subscripts  $i$  and  $s$  denote the incoming and scattered portions of the fields respectively. The subscript 1 denotes the fields inside the sphere. By filling out the fields given by equations 58-61, 65 and 66 we obtain

$$\begin{aligned}
j_n(mx)c_n + h_n^{(1)}(x)b_n &= j_n(x) \\
\mu[mxj_n(mx)]'c_n + \mu_{int}[xh_n^{(1)}(x)]'b_n &= \mu_{int}[xj_n(x)]' \\
\mu mj_n(mx)d_n + \mu_{int}h_n^{(1)}(x)a_n &= \mu_{int}j_n(x) \\
[mxj_n(mx)]'d_n + m[xh_n^{(1)}(x)]'a_n &= m[xj_n(x)]'
\end{aligned} \tag{68}$$

Where the prime denotes the derivative to the argument of the concerned Bessel function.  $m_s$  Is the reflective index of the sphere,  $m$  the relative reflective index of the sphere to it's surrounding and  $m_p$  the reflective index of the surroundings.  $x$  Is the size parameter of the particle with  $a$  the radius of the particle wherefor

$$x = ka = \frac{2\pi m_p a}{\lambda} \tag{69}$$

holds. By assuming  $\mu = \mu_{int}$  the solutions for this set of equations in terms of the expansion coefficients become:

$$\begin{aligned}
a_n &= \frac{m^2 j_n(mx)[xj_n(x)]' - j_n(x)[mxj_n(mx)]'}{m^2 j_n(mx)[xh_n^{(1)}(x)]' - h_n^{(1)}(x)[mxj_n(mx)]'} \\
b_n &= \frac{j_n(mx)[xj_n(x)]' - j_n(x)[mxj_n(mx)]'}{j_n(mx)[xh_n^{(1)}(x)]' - h_n^{(1)}(x)[mxj_n(mx)]'} \\
c_n &= \frac{j_n(x)[xh_n^{(1)}(x)]' - h_n^{(1)}(x)[xj_n(x)]'}{j_n(mx)[xh_n^{(1)}(x)]' - h_n^{(1)}(x)[mxj_n(mx)]'} \\
d_n &= \frac{mj_n(x)[xh_n^{(1)}(x)]' - mh_n^{(1)}(x)[xj_n(x)]'}{m^2 j_n(mx)[xh_n^{(1)}(x)]' - m^2 h_n^{(1)}(x)[mxj_n(mx)]'}
\end{aligned} \tag{70}$$

With these equations derived, we are now able to calculate the scattering matrix.

### 2.2.4 Mie Theory in Relation to the Scattering Matrix

With the electric and magnetic scattered fields known, we can start to link them to the scattering matrix. First we define  $\rho = kr$  and the functions  $\pi_n$  and  $\tau_n$  as

$$\pi_n = \frac{P_n^1}{\sin \theta} \quad (71)$$

$$\tau_n = \frac{dP_n^1}{d\theta} \quad (72)$$

which reduces the equations 47-50 for  $m = 1$  to

$$\mathbf{M}_{e1n} = -\sin(\phi)\pi_n(\cos \theta)z_n(\rho)\hat{\mathbf{e}}_\theta - \cos(\phi)\tau_n(\cos \theta)z_n(\rho)\hat{\mathbf{e}}_\phi \quad (73)$$

$$\mathbf{M}_{o1n} = \cos(\phi)\pi_n(\cos \theta)z_n(\rho)\hat{\mathbf{e}}_\theta - \sin(\phi)\tau_n(\cos \theta)z_n(\rho)\hat{\mathbf{e}}_\phi \quad (74)$$

$$\begin{aligned} \mathbf{N}_{e1n} = & \cos(\phi)n(n+1)\sin \theta\pi_n(\cos \theta)\frac{z_n(\rho)}{\rho}\hat{\mathbf{e}}_r \\ & + \cos(\phi)\tau_n(\cos \theta)\frac{[\rho z_n(\rho)]'}{\rho}\hat{\mathbf{e}}_\theta - \sin(\phi)\pi_n(\cos \theta)\frac{[\rho z_n(\rho)]'}{\rho}\hat{\mathbf{e}}_\phi \end{aligned} \quad (75)$$

$$\begin{aligned} \mathbf{N}_{o1n} = & \sin(\phi)n(n+1)\sin \theta\pi_n(\cos \theta)\frac{z_n(\rho)}{\rho}\hat{\mathbf{e}}_r \\ & + \sin(\phi)\tau_n(\cos \theta)\frac{[\rho z_n(\rho)]'}{\rho}\hat{\mathbf{e}}_\theta + \cos(\phi)\pi_n(\cos \theta)\frac{[\rho z_n(\rho)]'}{\rho}\hat{\mathbf{e}}_\phi \end{aligned} \quad (76)$$

$$(77)$$

Where the prime denotes the derivative to the argument of the concerned Bessel function. Let  $x = ka$  the size parameter of the particle with  $a$  the radius of the particle. The scattering coefficients are then given by

$$a_n = \frac{m^2 j_n(mx)[x j_n(x)]' - j_n(x)[mx j_n(mx)]'}{m^2 j_n(mx)[x h_n^{(1)}(x)]' - h_n^{(1)}(x)[mx j_n(mx)]'} \quad (78)$$

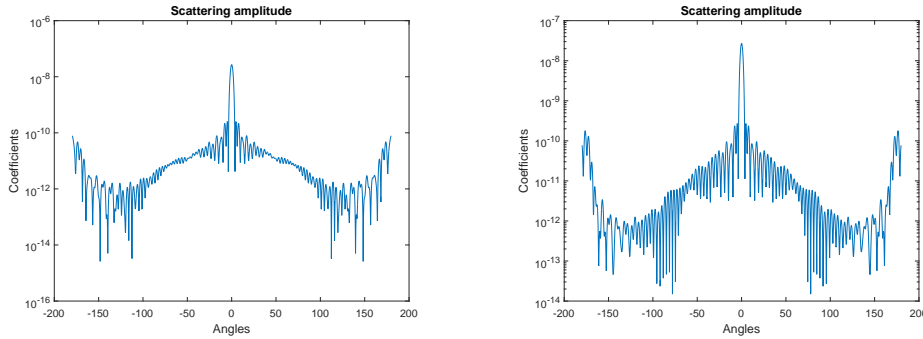
$$b_n = \frac{j_n(mx)[x j_n(x)]' - j_n(x)[mx j_n(mx)]'}{j_n(mx)[x h_n^{(1)}(x)]' - h_n^{(1)}(x)[mx j_n(mx)]'} \quad (79)$$

which completes the scattering coefficients  $S_1$  and  $S_4$  from equation 2;

$$S_1 = \frac{1}{-ik} \sum_{n=1}^{\infty} i^n \frac{2n+1}{n(n+1)} (a_n \tau_n(\cos \theta) + b_n \pi_n(\theta)) \quad (80)$$

$$S_4 = \frac{1}{-ik} \sum_{n=1}^{\infty} i^n \frac{2n+1}{n(n+1)} (a_n \pi_n(\cos \theta) + b_n \tau_n(\theta)) \quad (81)$$

The scatter coefficients  $S_1$  and  $S_4$  are calculated in Matlab. The source code is given in appendix D. In figure 1 plots are shown of  $|S_1|^2$  and  $|S_4|^2$  which are calculated for  $m = 1.68$ , the relative reflective index,  $a = 5 \cdot 10^{-6}$ , the radius of the scattering particles and  $\lambda = 532 \cdot 10^{-9}$  the wave length of the light. These parameters are chosen such to match the data of the experiment of Schepers.



(a) The scattering coefficient  $|S_1|^2$  as function of the angle.

(b) The scattering coefficient  $|S_4|^2$  as function of the angle.

Figure 1: Refraction coefficients as calculated by Mie theory with parameters  $m = 1.68$ ,  $a = 5 \cdot 10^{-6}$  and  $\lambda = 532 \cdot 10^{-9}$ .

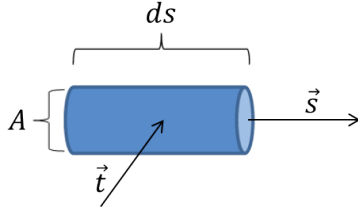
## 2.3 Light Propagation

In this section we derive the equations which describe light propagation. This will first be done in the form of an integral differential equation. Later on we will solve this equation. Because the solution is a implicit integral equation we split the solution in different orders. The work of Ishimaru<sup>[3]</sup> will be followed and extended to higher orders.

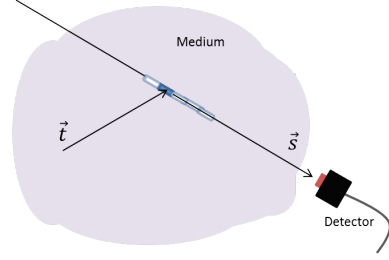
### 2.3.1 Differential Equation for Light Propagation

Let us consider a cilinder of arbitrary small length  $ds$  and negligible surface  $A$  with an incident light ray in the direction  $\mathbf{t}$  and scattered direction  $\mathbf{s}$  towards the detector as seen in figure 2a and 2b.

If we would denote the light intensity at a point  $\mathbf{r}$  propagating in the direction of  $\mathbf{s}$  by  $I(\mathbf{r}, \mathbf{s})$ , we can calculate the change of the intensity in the cilinder drawn in figure 2a in



(a) Representation of an incident ray which is scattered in a cylindrical volume with length  $ds$  from a direction  $\mathbf{t}$  to  $\mathbf{s}$ .



(b) Representation of the cylinder(s) of concern in a plasma.

the scattering medium of figure 2b. The change in the intensity is due to three effects: absorption, scattering and light sources. First we will consider each effect separately and then add them together.

The change in intensity at  $\mathbf{r}$  in the direction of  $\mathbf{s}$  is given by  $dI(\mathbf{r}, \mathbf{s})$ . There are  $\rho ds$  particles per square meter in the cylinder where  $\rho$  denotes the amount of particles per  $\text{m}^3$ . Per particle  $\sigma_a \cdot I$  is absorbed and  $\sigma_s \cdot I$  is scattered. Due to Lambert-Beer's law<sup>[7]</sup> the change in intensity due to absorption ( $dI_a(\mathbf{r}, \mathbf{s})$ ) is given by

$$\frac{dI_a(\mathbf{r}, \mathbf{s})}{ds} = -\rho\sigma_a I(\mathbf{r}, \mathbf{s}) \quad (82)$$

and the change in intensity due to light scattering away from the direction  $\mathbf{s}$  ( $dI_{s,a}(\mathbf{r}, \mathbf{s})$ ) is given by

$$\frac{dI_{s,a}(\mathbf{r}, \mathbf{s})}{ds} = -\rho\sigma_s I(\mathbf{r}, \mathbf{s}). \quad (83)$$

Let  $\varepsilon(\mathbf{r}, \mathbf{s})$  be a local light source which emits light in the direction of  $\mathbf{s}$  which doesn't come from scattering particles. Then the change in light intensity in the cylinder due to local sources ( $dI_{ls}(\mathbf{r}, \mathbf{s})$ ) is given by:

$$\frac{dI_{ls}(\mathbf{r}, \mathbf{s})}{ds} = \varepsilon(\mathbf{r}, \mathbf{s}). \quad (84)$$

The last possible change in the light intensity is due to light that has a direction  $\mathbf{t}$  scattered in the direction of  $\mathbf{s}$  ( $dI_{s,i}(\mathbf{r}, \mathbf{s})$ ). Equation 17 gives the total scattering for a particle away from direction  $\mathbf{t}$ . If we are interested in the intensity scattering towards the direction  $\mathbf{s}$ , the intensities at point  $\mathbf{r}$  scattering in direction  $\mathbf{s}$  should be taken into account. The light intensity which is scattered from direction  $\mathbf{t}$  to direction  $\mathbf{s}$  at point  $\mathbf{r}$  is given by  $p(\mathbf{s}, \mathbf{t}) \cdot I(\mathbf{r}, \mathbf{t})$ . The total change in intensity is therefore given by integrating over all possible incident directions which gives

$$\frac{dI_{s,i}(\mathbf{r}, \mathbf{s})}{ds} = \int_{4\pi} \frac{\rho\sigma_t}{4\pi} p(\mathbf{s}, \hat{\mathbf{t}}) I(\mathbf{r}, \hat{\mathbf{t}}) d\hat{\omega}. \quad (85)$$

By adding all these effects together, the total change in intensity is given by

$$\frac{dI(\mathbf{r}, \mathbf{s})}{ds} = -\rho\sigma_t I(\mathbf{r}, \mathbf{s}) + \frac{\rho\sigma_t}{4\pi} \int_{4\pi} p(\mathbf{s}, \hat{\mathbf{t}}) I(\mathbf{r}, \hat{\mathbf{t}}) d\hat{\omega} + \varepsilon(\mathbf{r}, \mathbf{s}) \quad (86)$$

This is the equation which will be the basis for the rest of the light propagation theory.

### 2.3.2 Diffuse Light Intensity

From equation 86 it is clear that the light intensity is different for different places. To get some more physical insight of the situation, we will introduce two new identities; the diffuse intensity ( $I_d$ ) and the reduced intensity ( $I_r$ ). The part of the incident beam which is reduced due to scattering and absorption is called the reduced intensity and is given by

$$\frac{dI_r(\mathbf{r}, \mathbf{s})}{ds} = -\rho\sigma_t I_r(\mathbf{r}, \mathbf{s}). \quad (87)$$

Because the reduced intensity and the diffuse intensity together form the total intensity,  $I(\mathbf{r}, \mathbf{s}) = I_d(\mathbf{r}, \mathbf{s}) + I_r(\mathbf{r}, \mathbf{s})$  holds. When we combine this with equations 86 and 87 it follows that

$$\begin{aligned} \frac{dI_d(\mathbf{r}, \mathbf{s})}{ds} &= \frac{dI(\mathbf{r}, \mathbf{s})}{ds} - \frac{dI_r(\mathbf{r}, \mathbf{s})}{ds} \\ &= -\rho\sigma_t I(\mathbf{r}, \mathbf{s}) + \frac{\rho\sigma_t}{4\pi} \int_{4\pi} p(\mathbf{s}, \hat{\mathbf{t}}) I(\mathbf{r}, \hat{\mathbf{t}}) d\hat{\omega} + \varepsilon(\mathbf{r}, \mathbf{s}) - (-\rho\sigma_t I_r(\mathbf{r}, \mathbf{s})) \\ &= -\rho\sigma_t (I(\mathbf{r}, \mathbf{s}) - I_r(\mathbf{r}, \mathbf{s})) + \frac{\rho\sigma_t}{4\pi} \int_{4\pi} p(\mathbf{s}, \hat{\mathbf{t}}) (I_d(\mathbf{r}, \hat{\mathbf{t}}) + I_r(\mathbf{r}, \hat{\mathbf{t}})) d\hat{\omega} + \varepsilon(\mathbf{r}, \mathbf{s}) \\ &= -\rho\sigma_t I_d(\mathbf{r}, \mathbf{s}) + \frac{\rho\sigma_t}{4\pi} \left( \int_{4\pi} p(\mathbf{s}, \hat{\mathbf{t}}) I_d(\mathbf{r}, \hat{\mathbf{t}}) d\hat{\omega} + \int_{4\pi} p(\mathbf{s}, \hat{\mathbf{t}}) I_r(\mathbf{r}, \hat{\mathbf{t}}) d\hat{\omega} \right) + \varepsilon(\mathbf{r}, \mathbf{s}) \\ &= -\rho\sigma_t I_d(\mathbf{r}, \mathbf{s}) + \frac{\rho\sigma_t}{4\pi} \int_{4\pi} p(\mathbf{s}, \hat{\mathbf{t}}) I_d(\mathbf{r}, \hat{\mathbf{t}}) d\hat{\omega} + \varepsilon(\mathbf{r}, \mathbf{s}) + \varepsilon_r(\mathbf{r}, \mathbf{s}) \end{aligned} \quad (88)$$

where  $\varepsilon_r(\mathbf{r}, \mathbf{s}) = \frac{\rho\sigma_t}{4\pi} \int_{4\pi} p(\mathbf{s}, \hat{\mathbf{t}}) I_r(\mathbf{r}, \hat{\mathbf{t}}) d\hat{\omega}$ . This is the scattering from the reduced intensity which acts like a local source term from the scattering particles: this is the light coming from particles which has been scattered only once.

### 2.3.3 Integral Equation for the Diffuse Intensity

Because it is often easier for modeling to work with integral equations rather than differential equations, we will transform equation 88 into an integral equation. To this end assume  $\mathcal{E}(\mathbf{r}, \mathbf{s}) = \varepsilon(\mathbf{r}, \mathbf{s}) + \varepsilon_r(\mathbf{r}, \mathbf{s})$ . This reduces equation 88 to

$$\frac{dI_d(\mathbf{r}, \mathbf{s})}{ds} = -\rho\sigma_t I_d(\mathbf{r}, \mathbf{s}) + \frac{\rho\sigma_t}{4\pi} \int_{4\pi} p(\mathbf{s}, \hat{\mathbf{t}}) I_d(\mathbf{r}, \hat{\mathbf{t}}) d\hat{\omega} + \mathcal{E}(\mathbf{r}, \mathbf{s}) \quad (89)$$

which is a differential equation of the form

$$\frac{dy}{dx} + Py(x) = Q(x) \quad (90)$$

where  $y = I_d(\mathbf{r}, \mathbf{s})$ ,  $x = s$ ,  $P = \rho\sigma_t$  and  $Q = \frac{\rho\sigma_t}{4\pi} \int_{4\pi} p(\mathbf{s}, \hat{\mathbf{t}}) I_d(\mathbf{r}, \hat{\mathbf{t}}) d\hat{\omega} + \mathcal{E}(\mathbf{r}, \mathbf{s})$ . Because  $P$  is a scalar,  $\int P dx = \int \rho\sigma_t ds = \tau$  always exists and thus we can use the method of the integrating factor to solve this differential equation. Multiplying both sides of equation 90 by  $\exp(\int^x P dx)$  gives

$$e^{\int^x P dx} \frac{dy}{dx} + P \cdot e^{\int^x P dx} y(x) = e^{\int^x P dx} Q(x) \quad (91)$$

if and only if

$$\frac{d}{dx}(e^{\int^x P dx} y(x)) = e^{\int^x P dx} Q(x). \quad (92)$$

Integrating both sides gives

$$e^{\int^x P dx} y(x) = \int_{x_0}^x e^{\int^{x_1} P dx} Q(x_1) dx_1 + C. \quad (93)$$

Here  $C$  is an arbitrary constant which will be determined later by a boundary condition. Dividing this result by  $\exp(\int P dx)$  gives the result we we're looking for

$$y(x) = e^{-\int^x P dx} \int_{x_0}^x e^{\int^{x_1} P dx} Q(x_1) dx_1 + C e^{-\int^x P dx} \quad (94)$$

By going back to our earlier notation this implies

$$I_d(\mathbf{r}, \mathbf{s}) = C e^{-\tau} + e^{-\tau} \left[ \int_0^s e^{\tau_1} \frac{\rho\sigma_t}{4\pi} \left( \int_{4\pi} p(\mathbf{s}, \hat{\mathbf{t}}) I_d(\mathbf{r}_1, \hat{\mathbf{t}}) d\hat{\omega} + \mathcal{E}(\mathbf{r}_1, \mathbf{s}) \right) ds_1 \right] \quad (95)$$

where  $\tau = \int_0^s \rho\sigma_t ds$  and  $\tau_1 = \int_0^{s_1} \rho\sigma_t ds$ . Let  $\mathbf{r}_0$  be the point of incidence. This implies  $I_d(\mathbf{r}_0, \mathbf{s}) = 0$  because  $\mathbf{s}$  is the direction of incidence here. There might be diffuse light at  $\mathbf{r}_0$  but this will be in an other direction (for example  $-\mathbf{s}$ ). Furthermore, at  $\mathbf{r}_0$  the optical distance  $\tau$  equals zero. By applying this to equation 95 we obtain:



$$0 = Ce^0 + e^{-0} \int_0^0 e^{\tau_1} \frac{\rho\sigma t}{4\pi} \int_{4\pi} p(\mathbf{s}, \hat{\mathbf{t}}) I_d(\mathbf{r}_1, \hat{\mathbf{t}}) d\hat{\omega} + \mathcal{E}(\mathbf{r}_1, \mathbf{s}) ds_1 = C. \quad (96)$$

So the integral equation we were looking for is given by

$$I_d(\mathbf{r}, \mathbf{s}) = \int_0^s e^{-(\tau-\tau_1)} \left[ \frac{\rho\sigma t}{4\pi} \int_{4\pi} p(\mathbf{s}, \hat{\mathbf{t}}) (I_d(\mathbf{r}_1, \hat{\mathbf{t}}) + I_r(\mathbf{r}_1, \hat{\mathbf{t}})) d\hat{\omega} + \varepsilon(\mathbf{r}_1, \mathbf{s}) \right] ds_1 \quad (97)$$

Because this equation is an implicit integral equation, it is not straight forward to obtain  $I_d$ . Therefore we will use a new approach in the next section.

### 2.3.4 Order Approach for the Diffuse Intensity

As seen in equation 97 the diffuse intensity is given by an implicit integral equation. In order to simplify this, we will consider all the orders of the diffuse intensity. We define the  $i^{\text{th}}$  order of the diffuse intensity as the light which has been scattered  $i - 1$  times. Light which has been scattered 0 times is assumed to be the reduced intensity. With this we can write

$$I_d(\mathbf{r}, \mathbf{s}) = \sum_{i=1}^{\infty} I_d^i(\mathbf{r}, \mathbf{s}) \quad (98)$$

where  $I_d^i(\mathbf{r}, \mathbf{s})$  is the  $i^{\text{th}}$  order of the diffuse intensity and  $I_d^0(\mathbf{r}, \mathbf{s}) = I_r(\mathbf{r}, \mathbf{s})$ . If we now substitute equation 98 into equation 97 we obtain

$$\begin{aligned} \sum_{i=1}^{\infty} I_d^i(\mathbf{r}, \mathbf{s}) &= \int_0^s e^{-(\tau-\tau_1)} \left[ \frac{\rho\sigma t}{4\pi} \int_{4\pi} p(\mathbf{s}, \hat{\mathbf{t}}) (\sum_{i=1}^{\infty} (I_d^i(\mathbf{r}_1, \hat{\mathbf{t}})) + I_r(\mathbf{r}_1, \hat{\mathbf{t}})) d\hat{\omega} + \varepsilon(\mathbf{r}_1, \mathbf{s}) \right] ds_1 \\ &= \int_0^s e^{-(\tau-\tau_1)} \left[ \frac{\rho\sigma t}{4\pi} \int_{4\pi} p(\mathbf{s}, \hat{\mathbf{t}}) \sum_{i=0}^{\infty} (I_d^i(\mathbf{r}_1, \hat{\mathbf{t}})) d\hat{\omega} + \varepsilon(\mathbf{r}_1, \mathbf{s}) \right] ds_1 \\ &= \int_0^s e^{-(\tau-\tau_1)} \left[ \frac{\rho\sigma t}{4\pi} \int_{4\pi} \sum_{i=0}^{\infty} (p(\mathbf{s}, \hat{\mathbf{t}}) I_d^i(\mathbf{r}_1, \hat{\mathbf{t}})) d\hat{\omega} + \varepsilon(\mathbf{r}_1, \mathbf{s}) \right] ds_1 \end{aligned} \quad (99)$$

Because the incident intensity forms an upper bound for the diffuse intensity and 0 is a lower bound, the integration and summation are also bounded thus the Weierstrass-M test<sup>[8]</sup> applies. This implies that the summation is uniformly convergent and the integrations and summation may be switched (see appendix A for a formal prove):

$$\sum_{i=1}^{\infty} I_d^i(\mathbf{r}, \mathbf{s}) = \int_0^s e^{-(\tau-\tau_1)} \left[ \frac{\rho\sigma t}{4\pi} \sum_{i=0}^{\infty} \left( \int_{4\pi} p(\mathbf{s}, \hat{\mathbf{t}}) I_d^i(\mathbf{r}_1, \hat{\mathbf{t}}) d\hat{\omega} \right) + \varepsilon(\mathbf{r}_1, \mathbf{s}) \right] ds_1 \quad (100)$$

By using the same argument again, we can switch the summation and integration once more to obtain

$$\sum_{i=1}^{\infty} I_d^i(\mathbf{r}, \mathbf{s}) = \sum_{i=0}^{\infty} \left( \int_0^s e^{-(\tau-\tau_1)} \left[ \frac{\rho\sigma_t}{4\pi} \int_{4\pi} p(\mathbf{s}, \hat{\mathbf{t}}) I_d^i(\mathbf{r}_1, \hat{\mathbf{t}}) d\hat{\omega} \right] ds_1 \right) + \int_0^s e^{-(\tau-\tau_1)} \varepsilon(\mathbf{r}_1, \mathbf{s}) ds_1 \quad (101)$$

From this result we can split the summation into it's components:

$$I_d^{i+1}(\mathbf{r}, \mathbf{s}) = \begin{cases} \int_0^s e^{-(\tau-\tau_1)} \left[ \frac{\rho\sigma_t}{4\pi} \int_{4\pi} p(\mathbf{s}, \hat{\mathbf{t}}) I_r(\mathbf{r}_1, \hat{\mathbf{t}}) d\hat{\omega} \right] ds_1 + \int_0^s e^{-(\tau-\tau_1)} \varepsilon(\mathbf{r}_1, \mathbf{s}) ds_1 & \text{if } i = 0 \\ \int_0^s e^{-(\tau-\tau_1)} \left[ \frac{\rho\sigma_t}{4\pi} \int_{4\pi} p(\mathbf{s}, \hat{\mathbf{t}}) I_d^i(\mathbf{r}_1, \hat{\mathbf{t}}) d\hat{\omega} \right] ds_1 & \text{if } i \geq 1 \end{cases} \quad (102)$$

Because the summation from equation 101 is convergent, the definition of convergence holds. This definition states:  $\forall \epsilon > 0 \exists n_0 \in \mathbb{N} \forall n \geq n_0 : |f_n - L| < \epsilon$ . Thus when a certain precision is desired, a  $n \in \mathbb{N}$  exists so that this precision can be achieved when  $I_d^i(\mathbf{r}, \mathbf{s})$  is known for all  $0 \leq i \leq n$ . Thus taking higher orders of  $I_d^i$  into account improves the precision.

### 3 Numerical Integration

When building a model, numerical simulation is often needed. For numerical problems, interpolation often is the basis for more complex theories, one example is numerical integration. In the next section we will start with properties of interpolation. after this we will consider Lagrange interpolation. Next the Newton-Cotes formula will be derived which will be the basis for numerical integration. For the derivations in this section the work of Kincaid and Cheney<sup>[4]</sup> and Fröberg<sup>[9]</sup> has been followed.

#### 3.1 Interpolation

Interpolation is a method for determining unknown values in between known values. This is often done by constructing polynomials which pass through the known values. This will be used for the next theorem.

Assume there are  $n + 1$  known coordinate pairs  $(x_i, y_i)$  with  $i = 0, 1, 2, \dots, n$  and  $x_0 < x_1 < \dots < x_n$  and we seek a polynomial  $p$  of the lowest possible degree which satisfies

$$p(x_i) = y_i \quad (0 \leq i \leq n). \quad (103)$$

The polynomial  $p$  then interpolates the given data. Less strictly said,  $p(x)$  is an approximation for  $y$  on  $D = (x_0, x_n)$ .

**Theorem 1.** *If  $x_0, x_1, \dots, x_n$  are distinct real numbers, then for arbitrary real numbers  $y_0, y_1, \dots, y_n$  there is a unique polynomial  $p_n$  with  $\deg(p_n) \leq n$  such that*

$$p_n(x_i) = y_i \quad (0 \leq i \leq n). \quad (104)$$

*Proof.* To prove this theorem both uniqueness and existence has to be proven. We will start with uniqueness.

Let  $p_n$  and  $q_n$  be two polynomials which satisfy the theorem. The composed polynomial  $(p_n - q_n)$  then should satisfy the relation  $(p_n - q_n)(x_i) = 0$  for every  $x_i$  with  $0 \leq i \leq n$  by definition. Then  $(p_n - q_n)(x_i)$  is at most of degree  $n$  because both polynomials are of most degree  $n$ . If  $(p_n - q_n)(x) \equiv 0$  the proof is done. Let us assume  $(p_n - q_n)(x)$  is not the zero polynomial, then  $(p_n - q_n)(x)$  has at most  $n$  zero's because it is at most of degree  $n$ . All  $n + 1$  distinct  $x_i$ 's are zero's of  $(p_n - q_n)(x)$  which is a contradiction. Thus  $(p_n - q_n)(x)$  is the zero polynomial.

To prove existence of a polynomial which satisfies the theorem we proceed inductively. For  $n = 0$  the constant polynomial  $p_0 = y_0$  satisfies the conditions and has degree of at most 0. Assume the polynomial  $p_{k-1}$  of degree at most  $k - 1$  has been obtained with  $p(x_i) = y_i$  we try to find  $p_k$  in the form

$$p_k(x) = p_{k-1} + c(x - x_0)(x - x_1) \cdots (x - x_{k-1}) \quad (105)$$

□

which is a polynomial of degree of at most  $k$ . Because  $p_k$  interpolates the data that  $p_{k-1}$  interpolates it holds that

$$p_k(x_i) = p_{k-1}(x_i) = y_i \quad (0 \leq i \leq k-1). \quad (106)$$

By invoking  $p(x_k) = y_k$  it follows

$$p_{k-1}(x_k) + c(x_k - x_0)(x_k - x_1) \cdots (x_k - x_{k-1}) = y_k. \quad (107)$$

This can be solved for  $c$  because all the factors multiplying  $c$  are not zero because all  $x_i$ 's are distinct. Thus  $p_k$  can be found. By induction  $p_n$  can be found.

### 3.2 Lagrange interpolation

Let us assume an interpolation polynomial  $p(x)$  expressed as

$$p(x) = y_0 L_0(x) + y_1 L_1(x) + \cdots + y_n L_n(x) = \sum_{k=0}^n y_k L_k(x) \quad (108)$$

We remark that  $p(x_i) = y_i$  thus using our polynomial expression it follows that  $y_i = \sum_{k=0}^n y_k L_k(x_i) = \sum_{k=0}^n y_k \delta_{ik}$  which implies  $L_k(x_i)$  must be of the form

$$L_i(x) = c(x - x_0)(x - x_1) \cdots (x - x_{i-1})(x - x_{i+1}) \cdots (x - x_n) = c \prod_{\substack{j=0 \\ j \neq i}}^n (x - x_j). \quad (109)$$

Thus substituting  $x = x_i$  gives  $L_i(x_i) = 1$  which implies

$$1 = c \prod_{\substack{j=0 \\ j \neq i}}^n (x_i - x_j). \quad (110)$$

So for  $c$  we find

$$c = \left( \prod_{\substack{j=0 \\ j \neq i}}^n (x_i - x_j) \right)^{-1} = \prod_{\substack{j=0 \\ j \neq i}}^n (x_i - x_j)^{-1} \quad (111)$$

which yields

$$L_k(x) = \prod_{\substack{j=0 \\ j \neq i}}^n \frac{x - x_j}{x_i - x_j}. \quad (112)$$

### 3.3 Newton-Cotes formula

When one is dealing with integrations, it is often desired to use numerical integration. Some integrals are nearly impossible to calculate analytical and some can not be expressed in elementary functions. To this end we will derive the Simpson's Rule, which is variant of the Newton-Cotes formulas.

Assuming the function  $y = f(x)$  has known values in the points  $x_0, x_1, \dots, x_{n-1}, x_n$  where the constant interval length is  $h$  and  $n$  is an even number. Using Lagrange Interpolation we find

$$P(x) = \sum_{k=0}^n L_k(x)y_k, \quad (113)$$

where

$$L_k(x) = \frac{(x - x_0)(x - x_1) \cdots (x - x_{k-1})(x - x_{k+1}) \cdots (x - x_{n-1})(x - x_n)}{(x_k - x_0)(x_k - x_1) \cdots (x_k - x_{k-1})(x_k - x_{k+1}) \cdots (x_k - x_{n-1})(x_k - x_n)}. \quad (114)$$

Because all the intervals are of length  $h$  each point can be written as  $x_k = x_0 + k \cdot h$ . Let  $x = x_0 + s \cdot h$  then  $\frac{dx}{ds} = h$  and

$$L_k = \frac{(s - 0)(s - 1) \cdots (s - k + 1)(s - k - 1) \cdots (s - n + 1)(s - n)}{(k - 0)(k - 1) \cdots (1)(-1) \cdots (k - n + 1)(k - n)}. \quad (115)$$

Integrating our function  $f(x)$  which is approximated by  $P(x)$  we find:

$$\int_{x_0}^{x_n} f(x) dx \approx \int_{x_0}^{x_n} P(x) dx = \int_{x_0}^{x_n} \sum_{k=0}^n L_k(x)y_k dx = nh \sum_{k=0}^n y_k \frac{1}{n} \int_0^n L_k ds. \quad (116)$$

For the sake of elegance we define  $C_k^n = \frac{1}{n} \int_0^n L_k ds$ . This reduces equation 116 to

$$\int_{x_0}^{x_n} f(x) dx \approx \int_{x_0}^{x_n} P(x) dx = nh \sum_{k=0}^n C_k^n y_k = (x_n - x_0) \sum_{k=0}^n C_k^n y_k. \quad (117)$$

The numbers  $C_k^n (0 \leq k \leq n)$  are called the Cotes numbers and equation 117 is called the Newton-Cotes formula. In the next section we will use these to derive the Simpson's Rule.

### 3.4 Simpson's Rule

Simpson's rule follows from Newton-Cotes formulas by setting  $n = 2$ . The corresponding Cotes numbers are

$$\begin{cases} C_0^2 &= \frac{1}{2} \int_0^2 \frac{(s-1)(s-2)}{(-1)(-2)} ds = \frac{1}{6} \\ C_1^2 &= \frac{1}{2} \int_0^2 \frac{s(s-2)}{1(-1)} ds = \frac{4}{6} \\ C_2^2 &= \frac{1}{2} \int_0^2 \frac{s(s-1)}{2 \cdot 1} ds = \frac{1}{6} \end{cases} \quad (118)$$

It then follows from equation 117

$$\int_{x_0}^{x_2} f(x) dx \approx \frac{(x_2 - x_0)}{6} (y_0 + 4y_1 + y_2) \quad (119)$$

This approximation is known as the Simpson's rule.

When using numerical methods one is often interested in the quality of the method. To this end we will perform an error analysis. Let us consider a 4 times continuous differentiable function  $f(x)$  in the interval  $(-h, h)$ .  $f(x)$  can then be approximated by a polynomial  $a_0 + a_1x + a_2x^2 + a_3x^3$  according to Taylor's Theorem around 0. The error of this approximation is given by  $x^4 \frac{f^{(4)}(\zeta)}{4!}$  with  $\zeta \in (-h, h)$ .

The error of Simpson's rule for this polynomial is given by

$$\begin{aligned} r(h) &= \frac{h-(-h)}{6} [f(-h) + 4f(0) + f(h)] - \int_{-h}^h f(x) dx \\ &= \frac{h}{3} (6a_0 + 2a_2h^2 + 2h^4 \cdot \frac{f^{(4)}(\zeta)}{4!}) - (2a_0h + \frac{2}{3}a_2h^3 + \frac{2}{5}h^5 \frac{f^{(4)}(\zeta)}{4!}) \\ &= (\frac{2}{3} - \frac{2}{5}) h^5 \frac{f^{(4)}(\zeta)}{4!} \\ &= \frac{4}{15} h^5 \cdot \frac{f^{(4)}(\zeta)}{4!} \end{aligned} \quad (120)$$

Let us consider an integral to be approximated by the Simpson's Rule which is taken over  $n$  equidistant points in an interval  $[a, b]$  where  $n$  is odd and  $n \geq 3$ . Let the  $n$  points be given by  $x_1, x_2, \dots, x_n$  and let  $x_{i+1} - x_i = h$  for all  $i = 1, 2, \dots, n-1$ , the distance between two points. The integral  $\int_a^b f(x) dx$  can then be written as

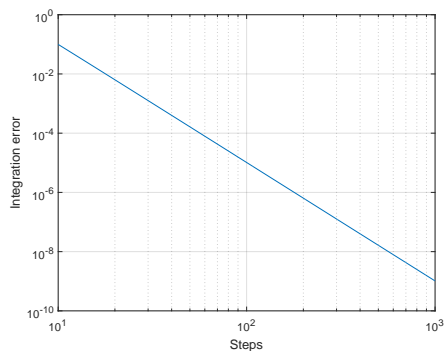
$$\int_a^b f(x) dx = \sum_{i=1}^{(n-1)/2} \int_{x_i}^{x_{i+2}} f(x) dx \quad (121)$$

because  $\bigcup_{i=1}^{n-1} [x_i, x_{i+1}] = [a, b]$ . Therefore the error of this integral is given by

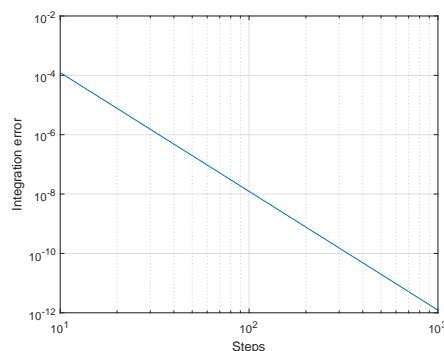
$$\begin{aligned} R(h) &= \sum_{i=1}^{(n-1)/2} r(h) \\ &= \sum_{i=1}^{(n-1)/2} \left( \frac{4}{15} \frac{f^{(4)}(\zeta)}{4!} \right) \\ &= \frac{4}{15} \cdot \frac{n-1}{2} \cdot h^5 \cdot \frac{f^{(4)}(\zeta)}{4!} \\ &= \frac{h^4}{180} \cdot (n-1) \cdot \frac{b-a}{n-1} \cdot f^{(4)}(\psi) \\ &= \frac{h^4}{180} (b-a) f^{(4)}(\psi) \end{aligned} \quad (122)$$

### 3.5 Application of the Simpson's Rule

In order to use the Simpson's Rule, a Matlab script has been written. It can be found in appendix B. The error found for the function  $f(x) = \exp(0.5 \cdot x)$  over the interval  $[0, 10]$  as function of the step size is displayed in figure 3a. The error found for the function  $g(x) = x \cdot \cos(0.1 \cdot x)$  over the interval  $[0, 5\pi]$  as function of the step size is displayed in figure 3b.



(a) The error of the approximation of the integral of  $\exp(0.5 \cdot x)$  as function of the amount of steps of the approximation



(b) The error of the approximation of the integral of  $x \cdot \cos(0.1 \cdot x)$  as function of the amount of steps of the approximation

Figure 3: Errors of the Simpson's Rule.

As can be seen in figure 3a and figure 3b the slope of the lines is 4 in both cases ( $\frac{(-1)-(-9)}{3-1} = 4$  and  $\frac{(-4)-(-12)}{3-1} = 4$  respectively). This corresponds with the theory which can be verified by taking the logarithme of equation 122. It then follows

$$\begin{aligned}
 \log(R(h)) &= \log\left(\frac{h^4}{180}(b-a)f^{(4)}(\psi)\right) \\
 &= \log(h^4) + \log\left(\frac{(b-a)}{180}f^{(4)}(\psi)\right) \\
 &= 4\log(h) + \log\left(\frac{(b-a)}{180}f^{(4)}(\psi)\right)
 \end{aligned} \tag{123}$$

for a certain  $\psi$  in the interval  $(a, b)$ . Thus a logarithmic plot should be a straight line with a slope of 4 and an offset of  $\frac{(b-a)}{180}f^{(4)}(\psi)$ .

For a function  $f$  whereof the fourth derivative is zero, the Simpson's rule converges exact. This can be seen by evaluating equation 122, which is the maximum error. The factor  $f^{(4)}(\psi)$  is zero for such a function, so the maximum error is zero. With this result we have an additional feature to check the validity of the Matlab script for the Simpson's Rule.

Let us consider the functions  $f_0(x) = 7$ ,  $f_1(x) = x$ ,  $f_2(x) = 2x^2$ ,  $f_3(x) = 0.25x^3$  and  $f_4(x) = 0.1x^4$  which are integrated over the interval  $[1, 5]$ . The functions are numerical evaluated in the points  $x = 1, 2, 3$  and  $x = 1, 2, 3, 4, 5$  for the Simpson's Rule. Table 1

Table 1: Table of the error made by the implemented Simpson's rule for different functions and different discretization steps.

	$f_0(x) = 7$	$f_1(x) = x$	$f_2(x) = 2x^2$	$f_3(x) = 0.25x^3$	$f_4(x) = 0.1x^4$
Analytical values	28	12	82.666	39	62.48
Simpson's values for 3 points estimate.	28.000	12.000	82.666	39.000	63.3333
Error	0	0	0	0	0.853
Simpson's values for 5 points estimate.	28.000	12.000	82.666	39.000	62.5333
Error	0	0	0	0	0.0533

shows the analytical solution for the integral  $\int_1^5 f(x) dx$ , the value that Simpson's Rule provide and the error.

We see that our expectation holds. The errors for the numeric integration of the polynomials are all zero but for the polynomial of degree 4. This is because  $f_4^{(4)}(\psi) = 1 \neq 0$  thus a maximum non-zero error exists. By equation 122, the errors should be equal or smaller than  $\frac{h^4}{180}(b-a)f^{(4)}(\psi)$  which are  $2.4 * \frac{16}{45} \approx 0.85333$  and  $\frac{2.4}{45} \approx 0.05333$  for the 'three points Simpson' and the 'five points Simpson' respectively. The errors indeed satisfy this restrictions. With these results we will consider the script made for the Simpson's rule as correct. This will be used for numerical analyses in the next section.



## 4 Models

To show some practical applications of the theory of light scattering, a few models have been made. These will be discussed in this section.

### 4.1 Plane Wave Incident on a Plane-Parallel Medium

Let us consider a plane-parallel medium of thickness  $d$  with random particles as illustrated in figure 4. Both the medium and the incident light beam are considered to extend to infinity. Let  $F_0$  denote the flux of the plane wave right after incidence so that Fresnel reflections are taken into account already. We assume that all the light which is incident on the plane, is incident with the same angle  $\theta_i$  and that all the light is transmitted with an angle  $\theta_t$ . Both these angles are measured with the normal of the incident surface. In practice this is a realistic model if the maximum penetration depth ( $d$ ) is much smaller than the total length (in the  $x$  direction) of the medium. This is a typical model for the light penetration in the ocean where the ocean surface and the ocean bottom are both considered flat.

For convenience we will measure the optical distance by  $\tau = \rho\sigma_t z$  along the  $z$ -axis instead of  $\rho\sigma_t z \sec \theta_t$  along the wave propagation and we define  $\mu_t = \cos \theta_t$ . If we consider the incident light beam to be pointed in one well defined direction, as is the case of sunlight on the ocean surface due to the large distance between the earth and the sun, the reduced incident intensity becomes

$$I_r(\tau) = F_0 e^{(-\tau/\mu_t)} \delta(\omega - \omega_0). \quad (124)$$

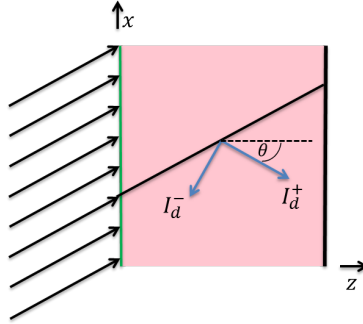


Figure 4: Illustration of an infinitely large Plane-Parallel medium with an infinite large incident light beam.

Where  $\delta(\omega - \omega_0)$  is the delta function of  $\omega$ , the integration variable which represents the angle, and  $\omega_0$ , which is the angle the light is heading in.

This model can be solved analytically if we are only interested in the first order light intensity. To this end, we define  $\mu = \cos \theta$  and note that the intensity  $I_{d+}$  is due to the

contributions of the reduced intensity in the range of  $0 \leq \theta \leq \pi/2$  ( $1 \geq \mu \geq 0$ ) and that  $I_{d-}$  is due to the contributions of the reduced intensity in the range of  $\pi/2 \leq \theta \leq \pi$  ( $0 \geq \mu \geq -1$ ) (forward and backward scattering). By substituting equation 124 in 102, assuming there are no local light sources (i.e.  $\varepsilon(r, s) = 0$ ) and noting that the optical path is measured along the  $z$ -axis instead of along the wave propagation, we obtain:

$$\begin{aligned}
I_{d+} = I_{d+}^1(\mathbf{r}, \mathbf{s}) &= \int_0^z \exp\left(-\frac{\tau-\tau_1}{\mu}\right) \left[ \frac{\rho\sigma_t}{4\pi} \int_{4\pi} p(\mathbf{s}, \hat{\mathbf{t}}) I_r(\mathbf{r}_1, \hat{\mathbf{t}}) d\hat{\omega} \right] ds_1 \\
&= \int_0^z \exp\left(-\frac{\tau-\tau_1}{\mu}\right) \cdot \left[ \frac{\rho\sigma_t}{4\pi} \int_{4\pi} p(\mathbf{s}, \hat{\mathbf{t}}) F_0 e^{(-\tau_1/\mu_t)} \delta(\hat{\omega} - \hat{\omega}_0) d\hat{\omega} \right] ds_1 \\
&= \int_0^z \exp\left(-\frac{\tau-\tau_1}{\mu}\right) \cdot \left[ \frac{\rho\sigma_t}{4\pi} p(\mathbf{s}, \boldsymbol{\omega}) F_0 e^{(-\tau_1/\mu_t)} \right] ds_1 \\
&= \int_0^z \exp\left(-\frac{\tau-\tau_1}{\mu} - \frac{\tau_1}{\mu_t}\right) \cdot \left[ \frac{\rho\sigma_t}{4\pi} p(\mathbf{s}, \boldsymbol{\omega}) F_0 \right] ds_1 \\
&= \int_0^\tau \exp\left(-\frac{\tau-\tau_1}{\mu} - \frac{\tau_1}{\mu_t}\right) d\left(\frac{\tau_1}{\mu}\right) \cdot \left[ \frac{1}{4\pi} p(\mathbf{s}, \boldsymbol{\omega}) F_0 \right] \quad (\star) \\
&= \frac{1}{\mu} \left(\frac{1}{\mu} - \frac{1}{\mu_t}\right)^{-1} \exp\left[-\frac{\tau-\tau_1}{\mu} - \frac{\tau_1}{\mu_t}\right]_0^\tau \cdot \left[ \frac{1}{4\pi} p(\mathbf{s}, \boldsymbol{\omega}) F_0 \right] \\
&= \frac{F_0}{4\pi\mu} \left(\frac{\mu_t}{\mu\mu_t} - \frac{\mu}{\mu\mu_t}\right)^{-1} \left(\exp\left(-\frac{\tau}{\mu_t}\right) - \exp\left(-\frac{\tau}{\mu}\right)\right) \cdot p(\mathbf{s}, \boldsymbol{\omega}) \\
&= \frac{F_0}{4\pi} \left(\frac{\mu_t}{\mu_t - \mu}\right) \left(\exp\left(-\frac{\tau}{\mu_t}\right) - \exp\left(-\frac{\tau}{\mu}\right)\right) \cdot p(\mathbf{s}, \boldsymbol{\omega})
\end{aligned} \tag{125}$$

where the integration substitution  $s_1 = \frac{\tau_1}{\mu\rho\sigma_t}$ ,  $\frac{ds_1}{d(\tau_1/\mu)} = \frac{1}{\rho\sigma_t}$  is made at step  $(\star)$ . The derivation of  $I_{d-}$  is analogue to the derivation of  $I_{d+}$  where the integration limits are  $s$  and  $d$ . The result is given by

$$I_{d-} = \frac{F_0}{4\pi} \left(\frac{\mu_t}{\mu_t - \mu}\right) \left(\exp\left(-\frac{\tau d}{\mu_t} + \frac{\tau d - \tau}{\mu}\right) - \exp\left(-\frac{\tau}{\mu_t}\right)\right) \cdot p(\mathbf{s}, \boldsymbol{\omega}) \tag{126}$$

where  $\tau_d = \tau(z = d) = \rho\sigma_t d$ . The result for  $\mu = \mu_t$  can be obtained by evaluating  $\lim_{\mu \rightarrow \mu_t} I_{d+}$ . It can also be obtained by substituting  $\mu = \mu_t$  in equation 125 in step  $(\star)$ . We will derive the result by the latter of the two, because this is the easier step. This results in

$$\begin{aligned}
I_{d+} &= \int_0^\tau \exp\left(-\frac{\tau-\tau_1}{\mu} - \frac{\tau_1}{\mu_t}\right) d\left(\frac{\tau_1}{\mu}\right) \cdot \left[ \frac{1}{4\pi} p(\mathbf{s}, \boldsymbol{\omega}) F_0 \right] \\
&= \int_0^\tau \exp\left(-\frac{\tau}{\mu_t}\right) d\left(\frac{\tau_1}{\mu_t}\right) \cdot \left[ \frac{1}{4\pi} p(\mathbf{s}, \boldsymbol{\omega}) F_0 \right] \\
&= \frac{\tau}{\mu_t} \exp\left(-\frac{\tau}{\mu_t}\right) \cdot \left[ \frac{1}{4\pi} p(\mathbf{s}, \boldsymbol{\omega}) F_0 \right] \\
&= \frac{\tau F_0}{4\pi\mu_t} \exp\left(-\frac{\tau}{\mu_t}\right) \cdot p(\mathbf{s}, \boldsymbol{\omega})
\end{aligned} \tag{127}$$

and analogue

$$I_{d-} = \frac{(\tau_d - \tau)F_0}{4\pi\mu_t} \exp\left(-\frac{\tau}{\mu_t}\right) \cdot p(\mathbf{s}, \boldsymbol{\omega}) \quad (128)$$

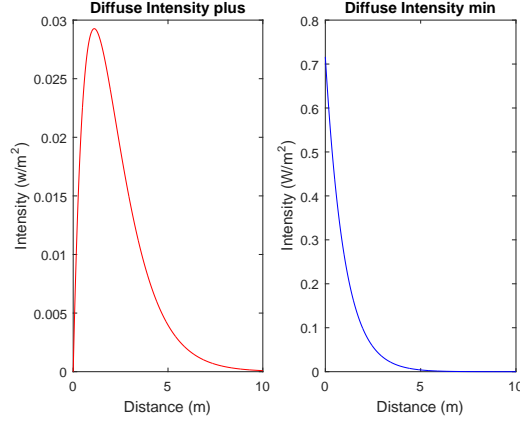


Figure 5: Simulated  $I_{d+}$  (Left) and  $I_{d-}$  (right) with parameters:  $\sigma_s = 0.1$ ,  $\sigma_a = 0.2$ ,  $\rho = 3$ ,  $\theta = \pi/6$ ,  $p(\mathbf{s}, \boldsymbol{\omega}) = 1$ ,  $d = 10$ ,  $F_0 = 1$  and  $\mu_t = 1$ .

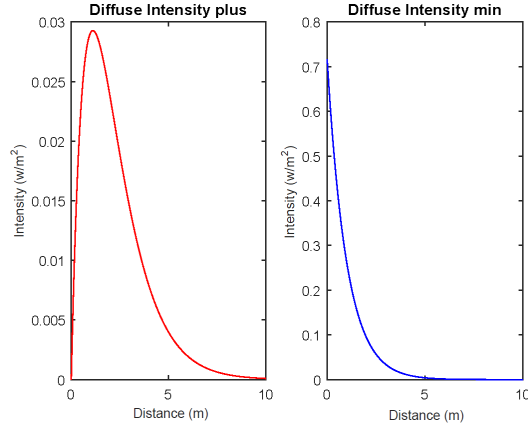
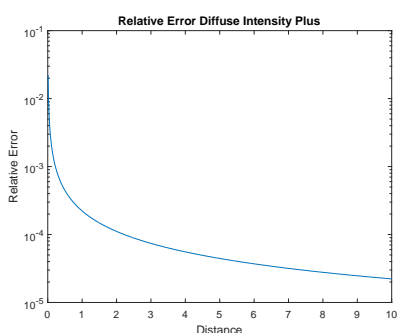


Figure 6: Analytically calculated  $I_{d+}$  (Left) and  $I_{d-}$  (right) with parameters:  $\sigma_s = 0.1$ ,  $\sigma_a = 0.2$ ,  $\rho = 3$ ,  $\theta = \pi/6$ ,  $p(\mathbf{s}, \boldsymbol{\omega}) = 1$ ,  $d = 10$ ,  $F_0 = 1$  and  $\mu_t = 1$ .

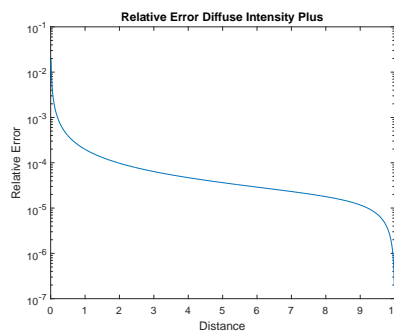
This model has also been programmed in Matlab. The source code can be found in appendix C.1. In figure 5 and 6 the diffuse intensities have been plotted. Figure 5 shows the intensities modelled in Matlab and 6 shows the analytical values. The  $I_{d+}$  graph shows the forward scattering as one would expect it to be. The forward scattering adds and thus increases as function of  $z$ , the distance. Because the incoming intensity drops due to Lambert-Beer's law, the forward scattering also decreases when deeper into the

medium. These two effects causes the visualised intensity. The  $I_{d-}$  graph shows the backscattered intensity which has the form one would suspect as well. The incoming intensity is the highest at  $z = 0$  thus the intensity which is scattered back is the highest at  $z = 0$  and drops when deeper into the medium because the incoming intensity drops. Additionally, the light scattered backwards adds, because it is traveling backwards, it will be at it's maximum at  $z = 0$  and it it's minimum at  $z = d$ . These two effects result in the displayed intensity.

The relative errors of the model in comparison to the analytical model, as shown in figure 7b, are small. The biggest relative error is  $10^{-2}$  at  $z = 0$  so the errors are less than or equal to 1% which is an acceptable value for experimental purposes.



(a) The relative error of the of the model of  $I_{d+}$  in comparison to the analytical value.



(b) The relative error of the of the model of  $I_{d-}$  in comparison to the analytical value.

Figure 7: Relative errors for the diffuse intensities simulated for 50000 points.

## 4.2 Plane Wave Incident on a Plane-Parallel Medium with a Finite Laser

This model is roughly the same as the model of the 'Plane Wave Incident on a Plane-Parallel Medium' which is given in the previous section. The main difference is the incident laser. In this example the laser is finite and we assume it to be a step function, the model has been visualized in figure 8. The model has been programmed in Matlab and the source code is given in appendix C.2. In figure 9 the modelled diffuse intensities have been plotted. The analysis is the same as the analysis of the 'Plane Wave Incident on a Plane-Parallel Medium' model. No significant differences, but a scaling of the intensity, are therefore expected.

If we compare figures 9 to figures 4, we see an increase in intensity for the model with the finite laser. This is because the intensity shown in graph 9 is the total intensity over the whole laser width. The intensity as shown in graph 4 is the intensity over one line. Because the used laser width is 5, we would expect a scaling by a factor 5. This is indeed true.

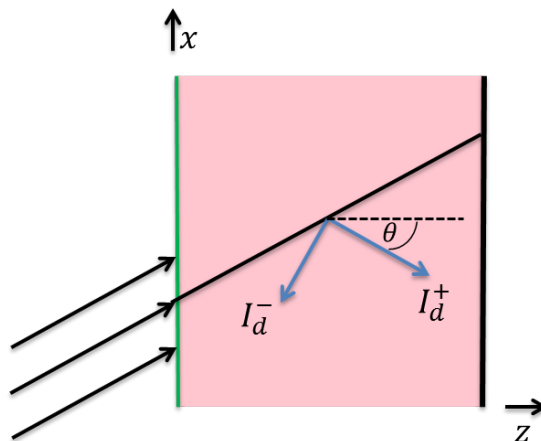


Figure 8: Illustration of an infinitely large Plane-Parallel medium with an finite incident light beam.

Figures 10 and 11 show the intensities for the angles  $\theta = \pi/6$  and  $\theta = \pi/3$ . The shape of the graphs are the same as the shape of the graph in figure 9. The only difference is a scaling of the intensity. This is because of the sightline which is used, which depends on  $\theta$ . For smaller  $\theta$  a bigger part of the illuminated medium is taken into account and therefore a bigger intensity will be found.

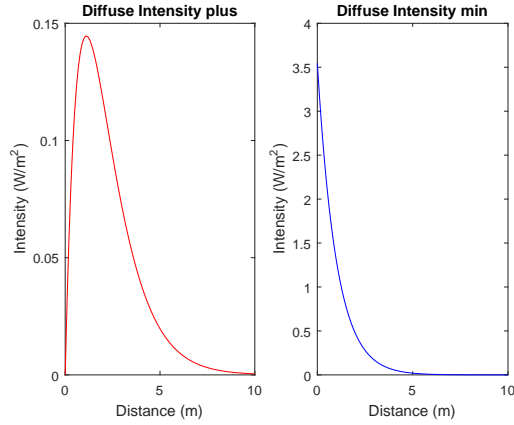


Figure 9:  $I_{d+}$  (Left) and  $I_{d-}$  (right) modelled in Matlab with parameters:  $\sigma_s = 0.1$ ,  $\sigma_a = 0.2$ ,  $\rho = 3$ ,  $\theta = 0$ ,  $p(\mathbf{s}, \boldsymbol{\omega}) = 1$ ,  $d = 10$ ,  $F_0 = 1, \mu_t = 1$  and the width of the laser is 5.

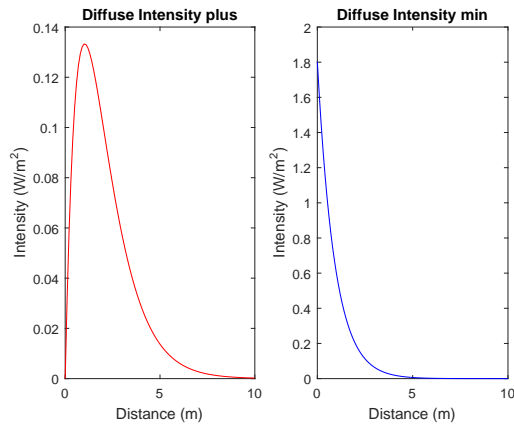


Figure 10:  $I_{d+}$  (Left) and  $I_{d-}$  (right) modelled in Matlab with parameters:  $\sigma_s = 0.1$ ,  $\sigma_a = 0.2$ ,  $\rho = 3$ ,  $\theta = \pi/6$ ,  $p(\mathbf{s}, \boldsymbol{\omega}) = 1$ ,  $d = 10$ ,  $F_0 = 1, \mu_t = 1$  and the width of the laser is 5.

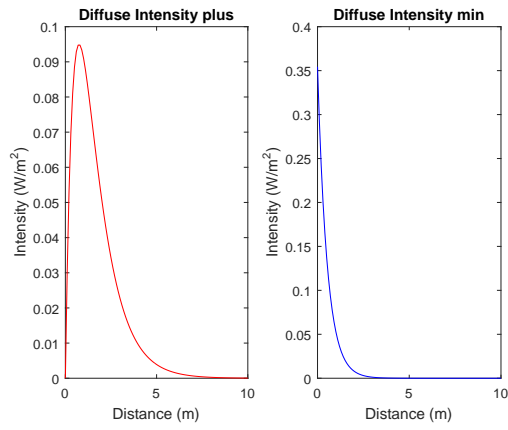


Figure 11:  $I_{d+}$  (Left) and  $I_{d-}$  (right) modelled in Matlab with parameters:  $\sigma_s = 0.1$ ,  $\sigma_a = 0.2$ ,  $\rho = 3$ ,  $\theta = \pi/3$ ,  $p(\mathbf{s}, \boldsymbol{\omega}) = 1$ ,  $d = 10$ ,  $F_0 = 1, \mu_t = 1$  and the width of the laser is 5.

### 4.3 Plane Wave Incident on a Circular Medium with a Flat Laser

In this section we will discuss a more experimental setup. Let us consider a cylinder with a relative small length (in the  $z$  direction) in comparison to the diameter (in the  $x$  and  $y$  direction) with an incident laser as visualized in figure 12. We are interested in the light along a sightline going through the center of the cylinder. This model could represent, for example, a dusty plasma which is illuminated by a laser. For that case, the line of sight is the direction in which the detector is measuring.

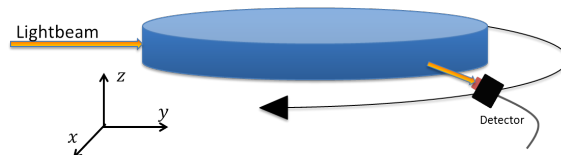


Figure 12: Setup for the situation of the 'Plane Wave Incident on a Circular Medium with a Flat Laser' model.

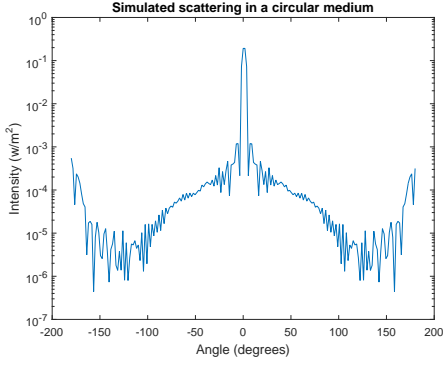
To make this situation a bit easier to model, we will assume that the cylinder is a circular sheet of spherical particles (in the  $x$  and  $y$  direction). The laser is assumed to be big enough in the  $z$  direction, to neglect boundary effects. Furthermore we assume that the laser is perfectly aligned along the sheet of particles and that the center of the laser heads through the center of the sheet. The laser's width is considered smaller than the diameter of the sheet. Furthermore, we assume that only the parallel components of the electric field of the light has a significant influence, so  $E_{\perp} = 0$ . With this assumption the phase function  $p(\mathbf{s}, \mathbf{t})$  becomes  $p(\alpha, \phi) = |S_1(\alpha, \phi)|^2$  where  $\phi$  is the angle of incidence and  $\alpha$  the angle the light is scattered. Because we assume a two dimensional situation with round particles, this phase function can be further reduced to  $p(\theta) = |S_1(\theta)|^2$  where  $\theta$  is the difference between the angle of incidence and the angle the light is scattered in. This is shown in graph 1a.

In order to use equation 102, we will need an other assumption. We will assume there are no local source terms in the plasma, so  $\varepsilon(r, s) = 0$ . When there are dust particles in the plasma which emit light, for example Phosphor particles,  $\varepsilon(r, s)$  should be chosen non-zero.

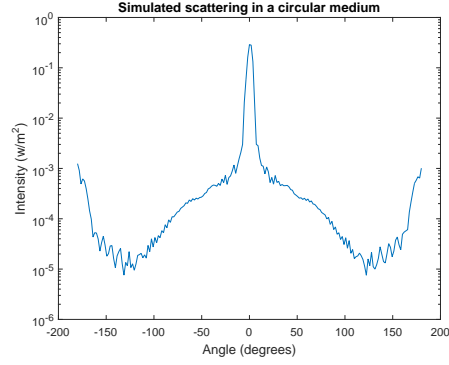
With these assumptions, a model can and has been made. It has been programmed in Matlab and is given in appendix C.3 along with the explanation of the working of the model. In section 4.4 a more realistic model has been described. If not stated otherwise, the results of the model of this section have been obtained by using the input parameters (AmountOfDiscretizationStepsCircle, thetaPoints, N) = (50, 100, 10) for the Matlab scripts.

A substantial amount of the light is scattered forward as can be seen in the figures 13. There is also a substantial amount of backscattering. For the first order scattering (figure 13a) one would expect a Mie scattering pattern. This Mie scattering is shown





(a) Light which has maximally scattered once.



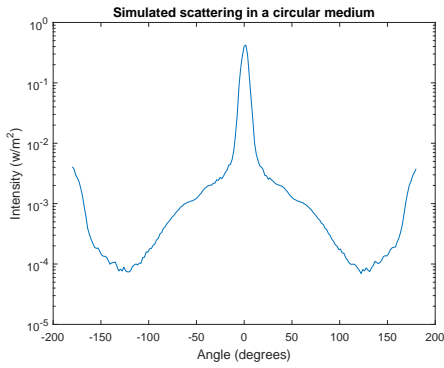
(b) Light which has maximally scattered twice.

Figure 13: The simulated intensity for a circular medium with parameters  $\rho = 10^{-12}$ ,  $\sigma_s = 1.7407 \cdot 10^{-10}$ ,  $\sigma_a = 6.0790 \cdot 10^{-22}$ ,  $F_0 = 1$ , width of the laser: 0.03, radius of the circular medium: 0.14,  $E_{\perp} = 0$  and the phase function as given by Mie Theory (figure 1a).

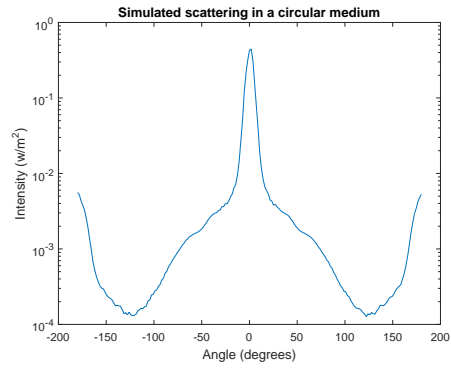
in figure 1a. The graph of figure 13a seems to show the same pattern. There are some difference though. The graph in figure 1a is smoother and contains more oscillations in comparison to the graph in figure 13a. This is most likely caused by too little discretization points. This hasn't been carried out yet due to the enormous amount of memory the model requires. By increasing the amount of discretization points, the implemented Simpson's rule becomes more accurate and the circular medium becomes 'rounder'. An other difference is the intensity. The simulated pattern shows a higher intensity because this represents light which has been scattered while the Mie pattern's 'intensity' can be seen as a scattering coefficient as function of the angle.

In figure 13b the intensity is shown for the light which has maximally scattered twice. We see that the graph evens out in comparison to the one time scattering. This due to the multiple scattering. The oscillations cancel out because all the the particles in the medium produces a Mie pattern in all directions. We would expect this effect to become more relevant for higher orders. In figure 14a and 14b the intensity is shown which has been scattered maximally five and maximally ten times respectively. We see that the graphs become smoother with increasing scattering orders.

In figure 15 graphs are shown for the same model as before. There has been one adjustment though, the scattering cross section has been decreased to  $\sigma_s = 1.2407 \cdot 10^{-10}$  so that the differences in the patterns become clearly visible. We see that the oscillations even out less for the situation with the lower scattering cross section. This is because the intensity decreases due to light scattering away from the direction it is heading in (Lambert-Beer), which is dependant of  $\sigma_s$ . For a lower cross section, less intensity is



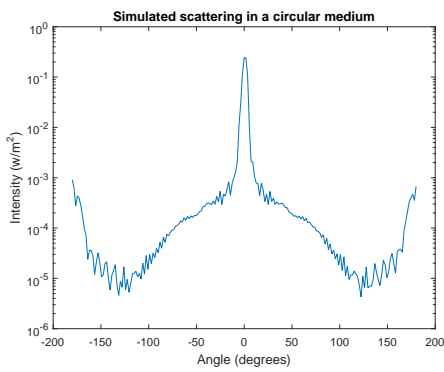
(a) Light which has maximally scattered five times.



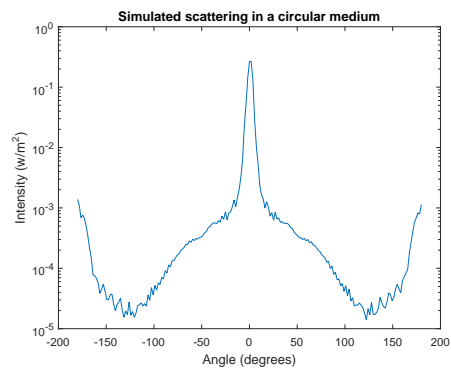
(b) Light which has maximally scattered ten times.

Figure 14: The simulated intensity for a circular medium with parameters  $\rho = 10^{-12}$ ,  $\sigma_s = 1.7407 \cdot 10^{-10}$ ,  $\sigma_a = 6.0790 \cdot 10^{-22}$ ,  $F_0 = 1$ , width of the laser: 0.03, radius of the circular medium: 0.14,  $E_{\perp} = 0$  and the phase function as given by Mie Theory (figure 1a).

scattered away so more light is left to scatter due to Mie scattering. Therefore it takes more Mie scattering before the oscillations even out. Because the scattering cross section is dependant on the size and the material of the particles, so does the scattering pattern. If, for example, one requires a certain scattering pattern then the choice of particles is important. This is because the scattering cross section is dependent on the size and the material of the particles due to the Mie theory.



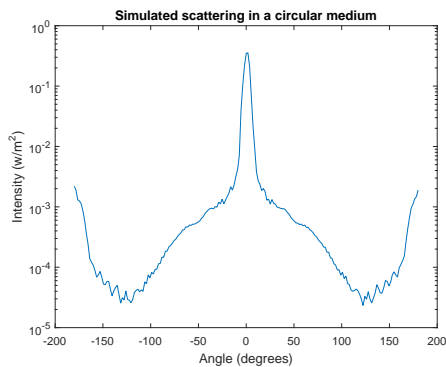
(a) Light which has maximally scattered twice.



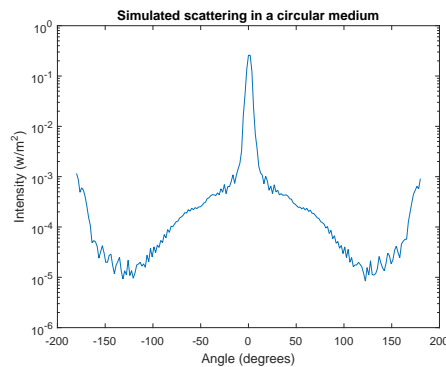
(b) Light which has maximally scattered ten times.

Figure 15: The intensity as would be measured by a detector due to light propagation in a dusty plasma. The parameters are  $\rho = 10^{-12}$ ,  $\sigma_s = 1.2407 \cdot 10^{-10}$ ,  $\sigma_a = 6.0790 \cdot 10^{-22}$ ,  $F_0 = 1$ , width of the laser: 0.03, radius of the circular medium: 0.14,  $E_{\perp} = 0$  and the phase function as given by Mie Theory (figure 1a).

Figures 16 and 17 show two more simulation results. These graphs also follow the patterns as discussed for the other graphs. When comparing figures 16a and 16b it clearly shows that a reduction of the scattering cross section  $\sigma_s$ , results in an increase in oscillations as expected.

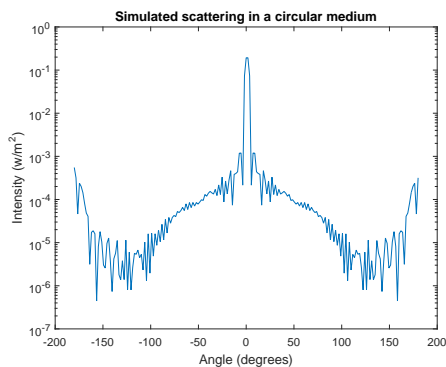


(a) Light which has maximally scattered three times with  $\sigma_s = 1.7407 \cdot 10^{-10}$ .

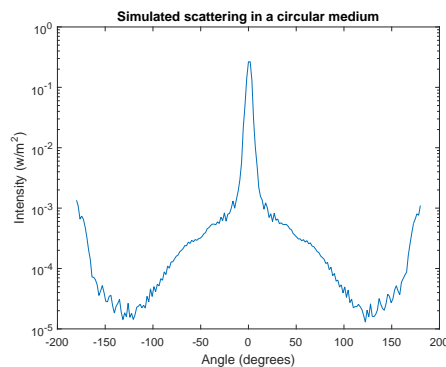


(b) Light which has maximally scattered three times with  $\sigma_s = 1.2407 \cdot 10^{-10}$ .

Figure 16: The simulated intensity for a circular medium with parameters  $\rho = 10^{-12}$ ,  $\sigma_a = 6.0790 \cdot 10^{-22}$ ,  $F_0 = 1$ , width of the laser: 0.03, radius of the circular medium: 0.14,  $E_{\perp} = 0$  and the phase function as given by Mie Theory (figure 1a).



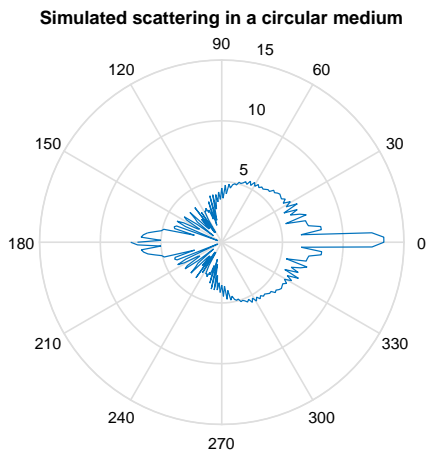
(a) Light which has maximally scattered once.



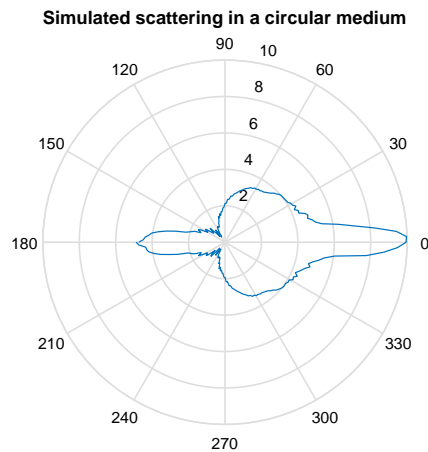
(b) Light which has maximally scattered five times.

Figure 17: The simulated intensity for a circular medium with parameters  $\rho = 10^{-12}$ ,  $\sigma_s = 1.2407 \cdot 10^{-10}$ ,  $\sigma_a = 6.0790 \cdot 10^{-22}$ ,  $F_0 = 1$ , width of the laser: 0.03, radius of the circular medium: 0.14,  $E_{\perp} = 0$  and the phase function as given by Mie Theory (figure 1a).

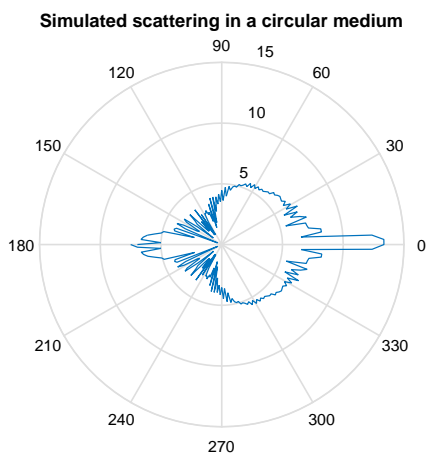
In figures 18 the intensities of figures 13a, 14a, 17a and 17b have been displayed in a logarithmic polar plot. These plots give a more visual representation of the scattering. It becomes clear that the oscillations indeed increase for a decrease of the scattering cross section. It also shows that an increase of the orders reduces the oscillations, in other words, the oscillations even out more for higher orders.



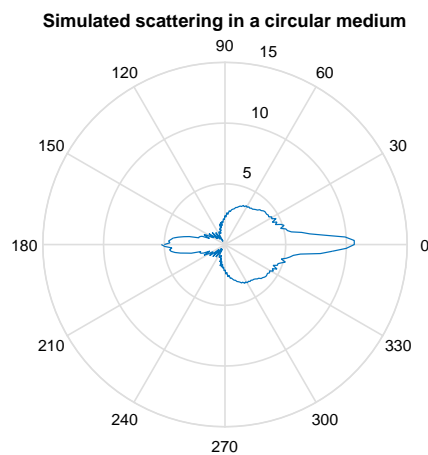
(a) Light which has maximally scattered once with  $\sigma_s = 1.7407 \cdot 10^{-10}$ .



(b) Light which has maximally scattered three times with  $\sigma_s = 1.7407 \cdot 10^{-10}$ .



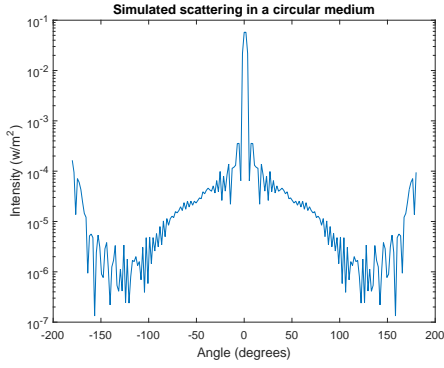
(c) Light which has maximally scattered once with  $\sigma_s = 1.2407 \cdot 10^{-10}$ .



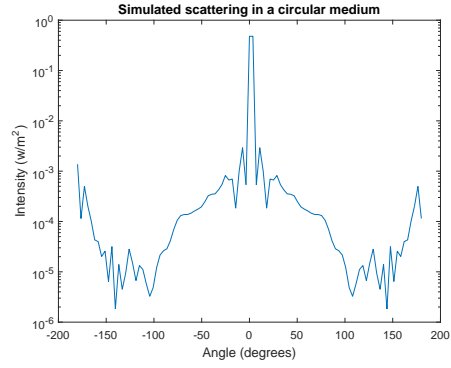
(d) Light which has maximally scattered three times with  $\sigma_s = 1.2407 \cdot 10^{-10}$ .

Figure 18: The simulated intensity in a polar plot for a circular medium with parameters  $\rho = 10^{-12}$ ,  $\sigma_a = 6.0790 \cdot 10^{-22}$ ,  $F_0 = 1$ , width of the laser: 0.03, radius of the circular medium: 0.14,  $E_{\perp} = 0$  and the phase function as given by Mie Theory (figure 1a).

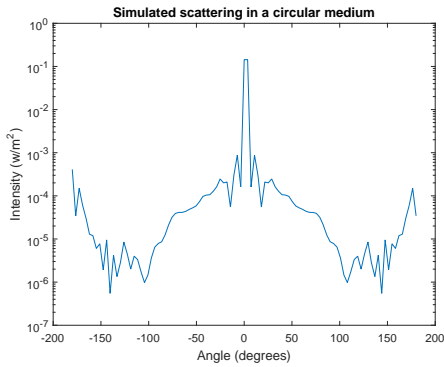
In figures 19 the results of the model are shown for various input parameters. These input parameters represent the amount of discretization points and therefore it is possible to discuss the convergence of the model. When comparing figure 13a with 19d, we see that in general the values of the latter are lower. On the other hand, we see that the values of graph 19c are higher than the values of 13a. This is most likely caused by the behaviour of the Mie pattern. The sampling from the oscillations in the Mie pattern, which happens in the numerical model, causes a biased value for the intensity. If for example the sampling happens on some maxima of the oscillations and not on the minima, it would produce an intensity higher than when the sampling would be done vice versa. An other reason for this difference in values is the implementation of how the circular medium is generated. For every value of the discretization step, it can occur that the matrix produced is not rotational symmetric. The fact that an element at the edge belongs to the circular medium is determined by numerical rounding. Therefore it can differ at maximum one element with the analytical result and thus the error is bounded. Therefore with an increase of the discretization steps, the influence of the medium being non rotational symmetric reduces. With these results we would therefore expect an converge for the results when the amount of discretization steps is increased.



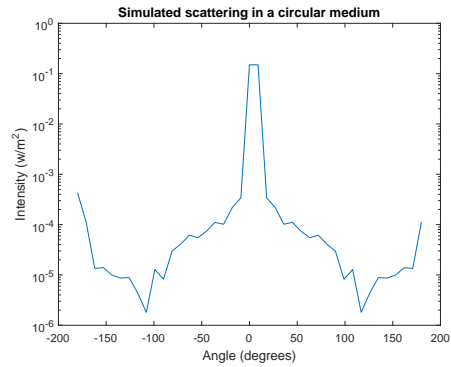
(a) Light which has maximally scattered once with input parameters (20,100,1).



(b) Light which has maximally scattered once with input parameters (50,50,1).



(c) Light which has maximally scattered once with input parameters (20,50,1).



(d) Light which has maximally scattered once with input parameters (20,20,1).

Figure 19: The intensity as would be measured by a detector due to light propagation in a dusty plasma. The parameters are  $\rho = 10^{-12}$ ,  $\sigma_s = 1.7407 \cdot 10^{-10}$ ,  $\sigma_a = 6.0790 \cdot 10^{-22}$ ,  $F_0 = 1$ , width of the laser: 0.03, radius of the circular medium: 0.14,  $E_{\perp} = 0$  and the phase function as given by Mie Theory (figure 1a).

#### 4.4 Improvements of the Plane Wave Incident on a Circular Medium with a Flat Laser

A more realistic model of the 'Plane Wave Incident on a Circular Medium with a Flat Laser' model would be to model the cylinder as stacked sheets of arbitrarily shaped particles. Furthermore the dimensions of the laser should be smaller than the dimensions of the cylinder. Choosing the  $E_{\perp}$  component of the electric field non-zero would make the situation more realistic as well.

Implementing these more realistic assumptions in Matlab should be straight forward as it is quite analogue to the programmed model. The only exception would be the shape of the particles. Matlab itself though, has some more problems with computing the model. The computational force needed for the programmed model is already enormous because it uses matrices which have up to 4 dimensions. For the more realistic model, six dimensional matrices and operations would be needed. To achieve a decent precision, each of these six dimensions would need enough elements which brings forth enormous matrices which causes memory issues.

One way to avoid the memory issues, also for the two dimensional case, is by using for-loops for the matrix operations. By doing this, the problem can shrink two dimensions (one in the two dimensional model). Although using for-loops is not advised in Matlab, no good other solutions are present. The problem therefore should be implemented differently if one wants to avoid for-loops. Implementing the models in C or C++ is also a good alternative.



## 5 Conclusion and Further Research

In this report we produced some models for the scattering of light in a dusty plasma. First the scattering at a particle was discussed. Here we saw that the scattering at spherical particles depends on the factors  $S_1$  and  $S_4$ . In order to calculate these factors, Mie theory was used. Mie theory provides a solution for the Maxwell equations associated with scattering at a particle. With knowledge of how scattering works, light propagation in a medium was analysed. Changes in the intensity of the light can be due to three effects: absorption, scattering and local sources (light emittance). While considering these effects, an integral differential equation for the propagation of light has been derived and solved. The solution to this differential equation is an implicit integral equation which was split into different orders. These different orders allowed for numerical analyses of some light propagation models.

The problems that were modelled are the 'Plane parallel medium' for both a laser with an infinite and finite diameter, and the 'Circular parallel medium'.

For the 'Plane parallel medium' a diffuse intensity has been found for both the forward and backward scattering. The intensity of the forward scattering behaved as an exponential function which increased just inside the medium and then decreased when further into the medium. This is caused by the addition of the forward scattering and the reduction by Lambert-Beer's law. The same argument holds for the backward scattering but the addition goes the other way. This is due to the reversed direction of the diffuse intensity.

A similar result holds for the 'Plane parallel medium with a finite laser'. The only difference is the angle dependency which induces a scaling in the intensity. Smaller  $\theta$  implies a bigger intensity. This is because a bigger part of the illuminated medium is taken into account.

For the model of the Circular medium we have seen that the Mie pattern is clearly visible for the first order scattering. For higher orders the oscillations of the Mie pattern even. This is due to multiple scattering which induces Mie scattering in all directions. It also became visible that a lower value for the scattering cross section causes the Mie pattern disappear slower. Because the scattering cross section is dependent on the size and the material of the particles, so does the scattering pattern.

Although the model of the Circular medium gives interesting results, it still has room for improvement. The memory usage of the model is enormous which makes it slow. If one is to improve this, higher orders could be calculated and the amount of discretization points could be increased which benefits the precision of the Simpson's Rule. An other improvement would be to extend the Circular medium model to three dimensions. By doing this the model would match Leroy's experiment better. Instead of assuming  $E_{\perp}$  to be zero, it could be assumed to be non-zero so that the light becomes polarized, which it is in most practical applications.

## A Changing the Order of Integration and Summation

The Theorem of the Weierstrass M-Test states<sup>[8]</sup>:

**Theorem 2.** *Suppose that  $\{f_n\}$  is a sequence of functions defined on  $D$  and suppose that  $\{M_n\}$  is a sequence of non negative real numbers such that  $|f_n(x)| \leq M_n$  for all  $x \in D$  and all  $n \in \mathbb{N}$ . If the series  $\sum M_k$  converges, then  $\sum |f_k|$  converges uniformly on  $D$  and hence,  $\sum f_k$  converges uniformly and absolutely on  $D$ .*

For a Riemann integrable function sequence, the following theory applies<sup>[8]</sup>:

**Theorem 3.** *Suppose  $\sum f_k$  is a series of Riemann integrable functions that converges uniformly to a function  $F$  on  $[a, b]$ . Then  $F$  is Riemann integrable and*

$$\int_a^b F(x) dx = \sum_{k=1}^{\infty} \int_a^b f_k(x) dx. \quad (129)$$

Furthermore, the next theorem holds<sup>[8]</sup>:

**Theorem 4.** *If a function  $f : [a, b] \rightarrow \mathbb{R}$  is continuous then  $f \in R[a, b]$ .*

So we can conclude that the order of integration and summation can be switched if each  $f_n$  is continuous (and thus Riemann integrable) and bounded.

If we apply this to

$$\sum_{i=1}^{\infty} I_d^i(\mathbf{r}, \mathbf{s}) = \int_0^s e^{-(\tau-\tau_1)} \left[ \frac{\rho\sigma t}{4\pi} \int_{4\pi} \sum_{i=0}^{\infty} (p(\mathbf{s}, \hat{\mathbf{t}}) I_d^i(\mathbf{r}_1, \hat{\mathbf{t}})) d\hat{\omega} + \varepsilon(\mathbf{r}_1, \mathbf{s}) \right] ds_1 \quad (130)$$

we may switch the order of integration and summation if  $p(\mathbf{s}, \hat{\mathbf{t}}) \cdot I_d^i(\mathbf{r}_1, \hat{\mathbf{t}})$  is continuous and bounded for all  $i = 0, 1, 2, 3, \dots$ . If both  $p(\mathbf{s}, \hat{\mathbf{t}})$  and  $I_d^i(\mathbf{r}_1, \hat{\mathbf{t}})$  are separately bounded and continuous the requirement is met. This will be proven next.

By definition (equation 98),  $I_d^i(\mathbf{r}_1, \hat{\mathbf{t}})$  is bounded. Because  $I_d^i(\mathbf{r}_1, \hat{\mathbf{t}}) \sim |\mathbf{E}|^2$  and  $\mathbf{E}$  is a solution to the wave equation,  $\mathbf{E}$  is continuous and therefore  $|\mathbf{E}|^2$  is continuous and therefor  $I_d^i(\mathbf{r}_1, \hat{\mathbf{t}})$  is continuous.

Because of the definition of the phase function (equation 10),  $p(\mathbf{s}, \hat{\mathbf{t}})$  is bounded and continuous. The continuity of  $p(\mathbf{s}, \hat{\mathbf{t}})$  is because the scattering matrix is continuous in it's entries which are continuous due to the Mie Theory.

Therefore the requirements are met so we can switch the order of integration and summation of equation 130 which gives.

$$\sum_{i=1}^{\infty} I_d^i(\mathbf{r}, \mathbf{s}) = \int_0^s e^{-(\tau-\tau_1)} \left[ \frac{\rho\sigma t}{4\pi} \sum_{i=0}^{\infty} \left( \int_{4\pi} p(\mathbf{s}, \hat{\mathbf{t}}) I_d^i(\mathbf{r}_1, \hat{\mathbf{t}}) d\hat{\omega} \right) + \varepsilon(\mathbf{r}_1, \mathbf{s}) \right] ds_1 \quad (131)$$

By using the same argument again, we can switch the summation and integration once more if  $e^{-(\tau-\tau_1)} \left[ \frac{\rho\sigma_t}{4\pi} \left( \int_{4\pi} p(\mathbf{s}, \hat{\mathbf{t}}) I_d^i(\mathbf{r}_1, \hat{\mathbf{t}}) d\hat{\omega} \right) \right]$  is continuous and bounded.

Because the integration  $\int_{4\pi} p(\mathbf{s}, \hat{\mathbf{t}}) I_d^i(\mathbf{r}_1, \hat{\mathbf{t}}) d\hat{\omega}$  is carried out over a finite interval with a bounded integrant, the result of the integration is bounded (and continuous). We know  $\tau = \int_0^s \rho\sigma_t ds \geq 0$  because  $s > 0$  and  $\tau \geq \tau_1$  because  $\tau_1 = \int_0^{s_1} \rho\sigma_t ds$  and  $s \geq s_1$ . This implies  $e^{-\tau} e^{-(\tau-\tau_1)} \leq 0$  and thus  $e^{-(\tau-\tau_1)}$  is bounded and continuous. Therefore  $e^{-(\tau-\tau_1)} \left( \frac{\rho\sigma_t}{4\pi} \int_{4\pi} p(\mathbf{s}, \hat{\mathbf{t}}) I_d^i(\mathbf{r}_1, \hat{\mathbf{t}}) d\hat{\omega} \right)$  is bounded and continuous. This implies we can switch the integration and summation once more to obtain

$$\sum_{i=1}^{\infty} I_d^i(\mathbf{r}, \mathbf{s}) = \sum_{i=0}^{\infty} \left( \int_0^s e^{-(\tau-\tau_1)} \left[ \frac{\rho\sigma_t}{4\pi} \int_{4\pi} p(\mathbf{s}, \hat{\mathbf{t}}) I_d^i(\mathbf{r}_1, \hat{\mathbf{t}}) d\hat{\omega} \right] ds_1 \right) + \int_0^s e^{-(\tau-\tau_1)} \varepsilon(\mathbf{r}_1, \mathbf{s}) ds_1. \quad (132)$$

## B Matlab Scripts for Simpson's Rule

The first script calculates and returns the desired approximation. It requires a row or column vector 'X' and the step size 'h' of the discretization .

```
function f = simpson(X,h)
%Function which uses the Simpson's Rule to integrate. If X is an array then
%h is the distance between two function values.

[lx wx]=size(X);

if (lx>=1) && (wx>=3) %X is a row vector
    if (mod(wx,2)==1) % There is an uneven amount of points, otherwise
        %Simpson cannot be used
        multi = 2*h*[1 repmat([4 2],[1 floor(wx/2)-1]) 4 1]/6; % Simpson's
        %weighting factors.
        X=X.';
        f=multi*X; %The actual integration
    end
else if (wx ==1) && (lx>=3) %X is a column vector
    if (mod(lx,2)==1)
        f=simpson(X.',h);
    else %uneven amount of points
        error('Not a compatible array.')
    end
else if (wx ==1) && (lx==1)
    f=sum(h*X);
else % X is no column nor a row vector
    error('Not a compatible array.')
end
end
end
end
```

The next script makes a logarithmic plot of the error of the approximation as function of the step size. For this example the function  $f(x) = \exp(0.5 \cdot x)$  is used to integrate. All functions which have an exact (known) elementary primitive can be used in fact as long as it isn't a polynomial of degree 3 or less, because these polynomials would be approximated with no error.

```
%This script will plot the error of Simpson's Rule as function of the step
%size in a logarithmic plot.
%The function f used to evaluate the error is given by f(x)=exp(0.5 x)

start = 0; %Begin of desired integral
finish = 10; %End of desired integral

exactValue = 2 * (exp(0.5 * finish)-exp(0.5 * start)); %Analytical value
%of the integral

AmountOfPoints = 10:2:1000; %The amount of points used to integrate over
```

```

%the interval, this determines the step size.
Y = zeros([1 length(AmountOfPoints)]); %Creation of an array so the
%for loop is evaluated faster

k=0; % Dummy variable to keep track of the array indices
for i = AmountOfPoints
    k=k+1;
    step = (finish-start)/i; %The integration step size, as said it depends
    %on the amount of points used to integrate.
    x=(start:step:finish); %The points at which the function f will be
    %evaluated
    y=exp(0.5 * x); %Dummy array which stores the function values at the
    %points of x
    Y(k)=simpson(y,step); % Keeping track of the values found by ...
        Simpson's Rule
end

loglog(AmountOfPoints, abs(Y-exactValue)) % Plotting of the error as
%function of the stepsize in a logarithmic plot
grid on %Lines in the plot are made visible for better readability
xlabel('Steps') %Label for the x-axis is set to 'Step size'
ylabel('Integration error') % Label for the y-axis is set to 'Integration ...
    error'

```

The next script does the same as the first script when the input is a vector. This script can have, in contrary to the former Simpson script, a matrix as input. The matrix should represent a discretized two dimensional integral with  $h$  the spacing between the elements in a row and  $k$  the spacing between the rows. The return value is the value of the double integral.

```

function f = simpson2(X,h,k)
%Function which uses the Simpson's Rule to integrate. If X is an array then
%only h is needed, the distance between two function values.
%If X is a matrix then h and k are needed where h is the spacing between the
%elements in a row and k the spacing between the rows.

[lx wx]=size(X);

if (lx>=1) && (wx>=3) %X is a row vector
    if (mod(wx,2)==1) % There is an uneven amount of points, otherwise
        %Simpson cannot be used
        multi = 2*h*[1 repmat([4 2],[1 floor(wx/2)-1]) 4 1]/6; % Simpson's
        %weighting factors.
        X=X.';
    if(lx>=3) && (mod(lx,2)==1) %2D matrix to be integrated
        temp = multi*X;
        multi = (2*k*[1 repmat([4 2],[1 floor(lx/2)-1]) 4 1]/6)';
        %Simpson's weighting factors.
        f=temp*multi; %The actual integration
    else if (mod(lx,2)==0)
        error('Not a compatible array.')
    else %1D matrix to be integrated

```

```

                f=multi*X; %The actual integration
            end
        end
    end
else if (wx ==1) && (lx>=3) %X is a colom vector
    if (mod(lx,2)==1) % There is an uneven amount of points,
        %otherwise Simpson cannot be used
        multi = 2*h*[1 repmat([4 2],[1 floor(wx/2)-1] 4 1)]/6;
        % Simpson's weigthing factors.
        f=multi*X; %The actual integration
    else % X is no colom nor a row vector
        error('Not a compatible array.')
    end
else if (wx ==1) && (lx==1)
    f=sum(h*X);
else
    error('Not a compatible array.')
end
end
end
end
end

```

The next script can be used to integrate in higher dimension and produce all the results the former Simpson scripts can. It has one drawback though, because of the general applicability it is harder to use correctly. The upside is, it can be used to integrate matrices of all dimension in all direction as often as desired. 'h' Is the distance between the elements in the direction of the input variable 'dim'. If an input is given for 'cumalitiveOption' the integration will be done cumulative. The script has been tested by comparing the results of this script to known analytical results and the results of the first script 'simpson'.

```

function f = simpson3(X,h,dim,cumalitiveOption)
%Function which uses the Simpson's Rule to integrate over the dimension dim.
%If X is a matrix then h is the distance between two function values along
%the dimension dim.

sizeX=size(X);
wx=sizeX(dim); %length of the matrix dimension to be integrated over,
%which needs to be uneven
if rem(wx,2)==0
    error('Not a compatible array');
end

amountOfDimension = length(sizeX);
arr=ones(1,amountOfDimension);
arr(dim)=sizeX(dim);
dimI=sizeX;
dimI(dim)=1;
multi = 2*h*[1 repmat([4 2],[1 floor(wx/2)-1] 4 1)]/6; %Simpson's weigthing
%factors
multi=reshape(multi, arr); %shaping the factors into the right dimension

```

```

multi= repmat(multi, [dimI 1]); %duplicating the factors for piecewise ...
multiplication

m=X.*multi; %matrix with the inputs multiplied by their weighting factor
if exist('cumalitiveOption') %if a third input is given the summation is done
    %cumulative
    f=cumsum(m, dim);
else
    f=sum(m, dim);
end
end
end

```

## C Matlab Models

The choice has been made to save in the Matlab scripts by using the save('file.mat') function. This allows for reusing calculated data. Because some scripts are slow, recalculating the data would be a waste. By minor adjustments the scripts given can load the data without the need for recalculating everything.

### C.1 Plane wave incident on a Plane-Parallel Medium

The first script calculates the values of  $I_{d+}$  and  $I_{d-}$  for the model of the plane wave incident on a plane-parallel medium in a point  $z$ . First the needed parameters are initialised. After this, the medium is discretized by 'm' points in the interval from 0 to 'z' and 'p' points in the interval 'z' to 'd' where 'm' and 'p' are forced to be uneven so that the Simpson's rule can be applied. After this the integral from 102, with equation 124 substituted, is calculated.

```

function [plus, min] = sModel(z, amountOfzDiscretizationSteps)
%function which returns the plus and minus diffuse intensity for an
%infinite large incident beam in a 2d 2 walls problem of infinite length

sigmaS = 0.1; %scattering cross section coefficient
sigmaA = 0.2; %absorbtion cross section coefficient
rho = 3; %particle density
theta = pi/6;
phase = 1; %phase function
d=10; % distance between the two walls
incidentIntensity = 1; %Incident density of the light, aka the incident
%intensity
source = 0; %The source function
mu0=1; %scalar

sigmaT = sigmaS + sigmaA; %total cross section coefficient
tau = rho * sigmaT * z; %optical path length
mu = cos(theta); % scalar for the amplitude

% m and p are forced to be uneven and m gets the fraction of discretization

```

```

% points comparable to the fraction z/d and p gets the fraction of
% discretization points comparable to the fraction 1-z/d and
m=round((tau/d)*amountOfzDiscretizationSteps);
if mod(m,2)==0
    m=m+1;
end
p=round(((d/mu0-tau)/d)*amountOfzDiscretizationSteps);
if mod(p,2)==0
    p=p+1;
end
step1=z/m;
step2=(d-z)/p;
tau1 = linspace(0,z,m);
tau2 = linspace(z,d,p);

reducedIntensityMatrix1 = exp(-tau1/mu0) * incidentIntensity ;
diffuseIntensityPlus = simpson(exp(-(tau-tau1)).*(rho*sigmaT/(4 * pi)) .* ...
    phase.*reducedIntensityMatrix1+source,step1);
reducedIntensityMatrix2 = exp(-tau2/mu0) * incidentIntensity ;
diffuseIntensityMin = simpson(exp(-(tau-tau2)).*(rho*sigmaT/(4 * pi)) .* ...
    phase.*reducedIntensityMatrix2+source,step2);
plus = diffuseIntensityPlus;
min = diffuseIntensityMin;

```

The next script uses the first model to make a plot of  $I_{d+}$  and  $I_{d-}$  as function of the distance. The parameter 'step' decides the smoothness of the plot that will be made and the parameter 'ModelAmountOfIntegrationPoints' decides the precision of the calculation of the model. The amount of points needed was determined by comparing the modelled results with the analytical results.

```

begin=0; %dimensions of the situation
finish=10;

step=0.01; %step size of the plot

ModelAmountOfIntegrationPoints=50000; %Points of integration for the model,
%this will decide it's accuracy

X=(begin:step:finish); %x values of the plot
Y1=zeros(1,length(X));
Y2=zeros(1,length(X));
for i=1:length(X)
    [y1 y2]=sModel(X(i),ModelAmountOfIntegrationPoints); % calculating the
    %y values of the plot
    Y1(i)=y1;
    Y2(i)=y2;
end

figure % create new figure
subplot(1,2,1) % first subplot
plot(X,Y1,'r') %plotting
xlabel('Distance (m)')

```



```

ylabel('Intensity (w/m^2)')
title('Diffuse Intensity plus') %labeling

subplot(1,2,2) % second subplot
plot(X,Y2,'b') %plotting
xlabel('Distance (m)')
ylabel('Intensity (W/m^2)')
title('Diffuse Intensity min') %labeling

```

## C.2 Plane wave incident on a Plane-Parallel Medium with a Flat Laser

The first script calculates the values of  $I_{d+}$  and  $I_{d-}$  for the model of the plane wave incident on a plane-parallel medium in a point  $z$ . First the needed parameters are initialised. After this, the medium is discretized by 'm' points in the interval from 0 to 'z' and 'p' points in the interval 'z' to 'd' where 'm' and 'p' are forced to be uneven so that the Simpson's rule can be applied. After this the laser model is discretized and forced to have an uneven amount of points. After this the integral from 102, with equation 124 substituted, is calculated over the two dimensional laser.

```

function [plus, minus] = modelLaserFlatPlasma(z, amountOfDiscretizationSteps)
%function which returns the plus and minus diffuse intensity for an
%infinite large incident beam in a 2d 2 walls problem of infinite length

sigmaS = 0.1; %scattering cross section coefficient
sigmaA = 0.2; %absorbtion cross section coefficient
rho = 3; %particle density
theta = 0;
phase = 1; %phase function
d=10; % distance between the two walls
LaserIntensity = 1; %Incident density of the light, aka the incident ...
    intensity
source = 0; %The source function
theta0=0;
mu0=cos(theta0); %scalar

sigmaT = sigmaS + sigmaA; %total cross section coefficient
tau = rho * sigmaT * z; %optical path length
mu = cos(theta); % scalar for the amplitude

%Dividing the interval into two parts and forcing it to have an uneven
%amount of discretization points
m=round((tau/d)*amountOfDiscretizationSteps);
if mod(m,2)==0
    m=m+1;
end
p=round(((d/mu0-tau)/d)*amountOfDiscretizationSteps);
if mod(p,2)==0
    p=p+1;
end
StepZ1=z/m;

```

```

StepZ2=(d-z)/p;
tau1 = linspace(0,z,m);
tau2 = linspace(z,d,p);
%Defining and discretizing the laser
startX = 0;
laserWidth = 5;
endX = startX+laserWidth;
steps=min([101,laserWidth/StepZ1,laserWidth/StepZ2]);
if mod(steps,2)==0
    steps=steps+1;
    incidentIntensityArray(1:steps)= LaserIntensity;
    StepX=(endX-startX)/(steps);
else
    incidentIntensityArray(1:steps)= LaserIntensity;
    StepX=(endX-startX)/(steps);
end

%Calculation of the diffuse plus intensity
reducedIntensityMatrix1 = ...
    bsxfun(@times,incidentIntensityArray',exp(-tau1/mu));
ToBeIntegratedMatrix1 = (bsxfun(@times,exp(-(tau-tau1)).*(rho*sigmaT/(4 * ...
    pi)) .* ...
    phase+source,reducedIntensityMatrix1))';
diffuseIntensityPlus = simpson2(ToBeIntegratedMatrix1,StepZ1,StepX);

%Calculation of the diffuse min intensity
reducedIntensityMatrix2 = ...
    bsxfun(@times,incidentIntensityArray',exp(-tau2/mu));
ToBeIntegratedMatrix2 = (bsxfun(@times,exp(-(tau-tau2)).*(rho*sigmaT/(4 * ...
    pi)) .* ...
    phase+source,reducedIntensityMatrix2))';
diffuseIntensityMin = simpson2(ToBeIntegratedMatrix2,StepZ2,StepX);

plus = diffuseIntensityPlus;
minus = diffuseIntensityMin;

```

The next script uses the first model to make a plot of  $I_{d+}$  and  $I_{d-}$  as function of the distance. The parameter 'step' decides the smoothness of the plot that will be made and the parameter 'ModelAmountOfIntegrationPoints' decides the precision of the calculation of the model.

```

begin=0; %dimensions of the situation
finish=10;

step=0.1; %step size of the plot (schaalt een op een met de tijd)

ModelAmountOfIntegrationPoints=5000; %Points of integration for the model,
%this will decide it's accuracy

X=(begin:step:finish); %x values of the plot
Y1=zeros(1,length(X));
Y2=zeros(1,length(X));

```

```

for i=1:length(X)
    [y1 y2]=modelLaserFlatPlasma(X(i),ModelAmountOfIntegrationPoints);
    % calculating the y values of the plot
    Y1(i)=y1;
    Y2(i)=y2;
end

figure % create new figure
subplot(1,2,1) % first subplot
plot(X,Y1,'r') %plotting
xlabel('Distance (m)')
ylabel('Intensity (W/m^2)')
title('Diffuse Intensity plus') %labeling

subplot(1,2,2) % second subplot
plot(X,Y2,'b') %plotting
xlabel('Distance (m)')
ylabel('Intensity (W/m^2)')
title('Diffuse Intensity min') %labeling

```

### C.3 Plane wave incident on a Circular Medium with a Flat Laser

The first script uses the scripts 'OrderCalculation' and 'ReducedIntensity' to calculate the diffuse intensity as a function of the angle. Which, for example, can be measured by a detector in a dusty plasma. This is done by integrating over the intensities along the lines passing through the middle of the circular medium in the direction outward perpendicular to the surface of the medium. These intensities needed are calculated by the script 'OrderCalculation'. It takes as input the order which needs to be calculated and uses the intensities of one order lower. The zeroth order is calculated by the script 'ReducedIntensity'. This script also calculates the shape of the medium. The script 'OrderCalculation' uses the script 'scattermatrix' given in section D to obtain the phase function.

The first script starts with initializing all the necessary parameters. After which the phase function and the zeroth order intensity are calculated. These are calculated in 'thetaPoints'\*2 + 1 and 'AmountOfDiscretizationStepsCircle'^2 points respectively. After this the orders are calculated up to order 'N', which are then added to the intensities of the previous orders. As last the integration over the lines through the middle of the medium are carried out to make an angular dependant plot.

```

function MainFunction(AmountOfDiscretizationStepsCircle,thetaPoints,N)

%Parameters
rho=1e12;
sigmaS=1.7407e-10;
sigmaA= 6.0790e-22;
LaserWidth=0.03;

```

```

straal=0.14;
plotting=0;

%Calculate Mie coefficients
scattermatrix(thetaPoints,plotting)

%Calculate reduced Intensity
ReducedIntensity(straal, LaserWidth, AmountOfDiscretizationStepsCircle, ...
    sigmaS, sigmaA, rho, plotting)

%Calculate all the orders of Intensity up to and including N
som=0;
for i=1:N
    OrderCalculation(i)
    fileLocation=['D:/Desktop/Technische natuurkunde/Jaar 3/Kwartiel 4'...
        '/BEP/Matlab-Script/Data/IntensityMatrix' num2str(i), '.mat'];
    load(fileLocation);
    som = som + IntensityMatrix;
    disp(i)
end

TotalIntensity=som;

theta=[];
load('D:/Desktop/Technische natuurkunde/Jaar 3/Kwartiel ...
    4/BEP/Matlab-Script/Data/Hoeken.mat');
angleInt=zeros([length(theta),1]);
angleStep = 360/length(theta);
theta = theta.*360./(2*pi);
thetaMiddle = (length(theta)+1)/2;
middle=(size(TotalIntensity,1)+1)/2;

%Integrating over all directions through the center of the circular medium
for i = 1:length(theta)
    angleInt(i)=simpson(TotalIntensity(middle,:,i),angleStep);
end

figure, semilogy(theta-180,(circshift(angleInt,thetaMiddle)))
title('Simulated scattering in a circular medium');
xlabel('Angle (degrees)');
ylabel('Intensity (w/m^2)');

%Because a Logarithmic polar plot doesn't work, we need to take the
%log of the data and add a constant to get all the values positive while
%remaining the shape of the data
a=abs(floor(min(log(angleInt))));
figure, polar((theta+180)./180.*pi,(circshift(log(angleInt),thetaMiddle))+a)
title('Simulated scattering in a circular medium');
end

```

The next script first checks if the input variable 'order' is non zero and an integer. It then loads the necessary data which is needed for the calculation. The input 'order' decides which order will be calculated by using the previous order. For 'order'= 0 the

script loads the reduced intensity and transforms it into a three dimensional array in which the directions are taken into account. This is the numerical equivalent for  $I_r(\mathbf{r}, \mathbf{s})$ . This matrix will be saved.

If 'order'= 1 the script loads the reduced intensity and if 'order' $\geq$  2 the script loads the previous order intensity. The data which has been loaded will be duplicated into a matrix with an additional dimension and multiplied with the Mie amplitude coefficients. After this the integration over the new dimension, will be carried out. This is the numerical equivalent of the integration of  $\frac{\rho\sigma_t}{4\pi} \int_{4\pi} p(\mathbf{s}, \hat{\mathbf{t}}) I_r(\mathbf{r}_1, \hat{\mathbf{t}}) d\hat{\omega}$ . After this the last integration is carried out over all the directions. The integration is done cumulative because the numerical equivalent of the factor  $e^{-(\tau-\tau_1)}$  can be calculated easily by a cumulative summation, which is done in the script 'simpson3' (Appendix B).

At last the new calculated order of the intensity is saved.

```
function OrderCalculation(order)
%Forces order to be non zero and an integer
if rem(order,1) ~= 0 || order<0
    error('Input requires a non-negative integer.')
end

%Load all the necessary data
load('D:/Desktop/Technische natuurkunde/Jaar 3/Kwartiel ...
    4/BEP/Matlab-Script/Data/PlacementGrid.mat');
load('D:/Desktop/Technische natuurkunde/Jaar 3/Kwartiel ...
    4/BEP/Matlab-Script/Data/Constants.mat');
w=num2cell(w);
[straal, sigmaS, sigmaA, rho, stepSizeCircle]=deal(w{:});
sigmaT=sigmaA+sigmaS;

load('D:/Desktop/Technische natuurkunde/Jaar 3/Kwartiel ...
    4/BEP/Matlab-Script/Data/reducingIntensityMatrix.mat');
S1=[];
load('D:/Desktop/Technische natuurkunde/Jaar 3/Kwartiel ...
    4/BEP/Matlab-Script/Data/S1.mat');
theta=[];
load('D:/Desktop/Technische natuurkunde/Jaar 3/Kwartiel ...
    4/BEP/Matlab-Script/Data/Hoeken.mat');
angleStep = 360/length(theta);
theta = theta.*360./(2*pi);
factor=0.1/simpson(S1,angleStep);

%Seperating cases
if(order==0)
    reducedIntensityMatrix=[];
    load('D:\Desktop\Technische natuurkunde\Jaar 3\Kwartiel ...
        4\BEP\Matlab-Script\Data\ReducedIntensity.mat')
    %Make the reduced Intensity a three dimensional matrix
    dimI=size(reducedIntensityMatrix);
    dimP = length(S1);
    IntensityMatrix= zeros([dimI dimP]);
```

```

IntensityMatrix(:,:,1)=reducedIntensityMatrix;
else if (order==1)
    reducedIntensityMatrix=[];
    load('D:\Desktop\Technische natuurkunde/Jaar 3/Kwartiel ...
        4/BEP/Matlab-Script/Data/ReducedIntensity.mat');
    dimI=size(reducedIntensityMatrix);
    dimP = length(S1);
    %Reshape the Mie coefficients and the Intensity so that element wise
    %multiplication can be applied
    reducedIntensityMatrix= repmat(reducedIntensityMatrix, [1 1 dimP]);
    S1=reshape(S1, [1 1 dimP]);
    S1=repmat(S1, [dimI 1]);
    %Analytical solution for the angle integration
    IntegratedPhasedMatrix = (factor*rho*sigmaT)/(4*pi)* S1 .* ...
        reducedIntensityMatrix;
    %Create matrices to make the for loop faster
    ReducedScatteredIntensityMatrix=zeros(size(IntegratedPhasedMatrix));
    TotalNewOrderIntensity=zeros(size(IntegratedPhasedMatrix));
    for i=1:length(theta)
        %Matrix to be integrated, this is the scattered matrix
        %multiplied by it's reducing factors e^(-(tau-taul))
        ReducedScatteredIntensityMatrix(:,:,i)=...
            reducedMatrix .* IntegratedPhasedMatrix(:,:,i);
        TotalNewOrderIntensity(:,:,i) = ...
            simpson3(ReducedScatteredIntensityMatrix(:,:,i), stepSizeCircle,2, 'cumulative');
    end
    IntensityMatrix=TotalNewOrderIntensity.*repmat(placementGrid, [1,1, dimP]);
else
    IntensityMatrix=[];
    fileLocation=strcat('D:\Desktop\Technische natuurkunde/Jaar ...
        3/Kwartiel 4/BEP/Matlab-Script/Data/IntensityMatrix', ...
        num2str(order-1), '.mat');
    load(fileLocation);
    [dimIx, dimIy, dimIz]=size(IntensityMatrix);
    dimP = length(S1);

    %Reshape the Mie coefficients and the Intensity so that element wise
    %multiplication can be applied

    S1=reshape(S1, [1 1 dimP]);
    S1=repmat(S1, [dimIx dimIy 1]);
    ToBeIntegratedPhasedMatrix=zeros([dimIx, dimIy, dimIz, dimP]);

    for i=1:dimP %multiplication with the right scattering factors
        multMatrix=repmat(IntensityMatrix(:,:,i), [1 1 dimP]);
        ToBeIntegratedPhasedMatrix(:,:,,i) = ...
            circshift((factor*rho*sigmaT)/(4*pi)* S1 .* multMatrix,-i,3);
    end

    IntegratedPhasedMatrix= ...
        simpson3(ToBeIntegratedPhasedMatrix, angleStep, 4);
    ReducedScatteredIntensityMatrix=zeros(size(IntegratedPhasedMatrix));
    TotalNewOrderIntensity=zeros(size(IntegratedPhasedMatrix));

```

```

for i=1:length(theta)
    %Matrix to be integrated, this is the scattered matrix
    %multiplied by it's reducing factors e^(-(tau-taul))
    ReducedScatteredIntensityMatrix(:, :, i) = ...
        reducedMatrix .* IntegratedPhasedMatrix(:, :, i);
    TotalNewOrderIntensity(:, :, i) = ...
        simpson3(ReducedScatteredIntensityMatrix(:, :, i), stepSizeCircle, 2, 'cumulative');
end
TotalNewOrderIntensity=reshape(TotalNewOrderIntensity, [dimIx ...
    dimIy dimIz]);
IntensityMatrix=TotalNewOrderIntensity.*repmat(placementGrid, [1, 1, dimP]);
end
end

fileLocation=strcat('D:/Desktop/Technische natuurkunde/Jaar 3/Kwartiel ...
    4/BEP/Matlab-Script/Data/IntensityMatrix', num2str(order), '.mat');
save(fileLocation, 'IntensityMatrix');

end

```

The next script calculates the reduced Intensity for a circular medium. It takes as input parameters the constants needed to calculate the reduced intensity. The 'AmountOfDiscretizationStepsCircle' parameter is forced to be uneven to make integrating over the circle easier which now can be done by using the script 'Simpson' (Appendix B). A circle is made by using the relation  $x^2 + y^2 \leq \text{'straal'}^2$ . Next the middle of the laser and the middle of the circle will be calculated. The reduced intensity of the laser will be calculated next and all the elements in the matrix which aren't in the width of the laser are set to zero. All the data which was necessary and the reduced intensity are then saved.

```

function ReducedIntensity(straal, LaserWidth, ...
    AmountOfDiscretizationStepsCircle, sigmaS, sigmaA, rho, plotting)

LaserIntensity = 1; %Incident density of the light, aka the incident ...
    intensity
sigmaT = sigmaS + sigmaA; %total cross section coefficient

%Forces the amount of discretization points to be uneven
if mod(AmountOfDiscretizationStepsCircle, 2) == 0
    AmountOfDiscretizationStepsCircle=AmountOfDiscretizationStepsCircle+1;
end

xvec = linspace(-straal, straal, AmountOfDiscretizationStepsCircle);
[x, y] = meshgrid(xvec, xvec);
bplacementGrid = x.^2 + y.^2 <= straal^2 ;

placementGrid = double(bplacementGrid);

stepSizeCircle=straal/AmountOfDiscretizationStepsCircle;

HalfSteps=round(LaserWidth/(2*stepSizeCircle));

```

```

CenterLaser=(length(placementGrid)+1)/2;
incidentIntensityArray=zeros(size(placementGrid));
incidentIntensityArray(CenterLaser-HalfSteps+1:CenterLaser+HalfSteps-1,:)= ...
    LaserIntensity;

%Calculating the reduced Intensity
reducedMatrix=cumsum(placementGrid,2).*placementGrid;
reducedMatrix=reducedMatrix .* stepSizeCircle .* rho .* sigmaT;
reducedIntensityMatrix = exp(-reducedMatrix);
save('D:/Desktop/Technische natuurkunde/Jaar 3/Kwartiel ...
    4/BEP/Matlab-Script/Data/reducingIntensityMatrix.mat','reducedMatrix');

%Setting all points outside the laser to zero
reducedIntensityMatrix(1:CenterLaser-HalfSteps,:)=0;
reducedIntensityMatrix(CenterLaser+HalfSteps:end,:)=0;
reducedIntensityMatrix=reducedIntensityMatrix .* incidentIntensityArray;

if(plotting)
    bp=placementGrid;
    bp(bp==0)=NaN;
    reducedIntensityMatrix=reducedIntensityMatrix .* bplacementGrid;
    mesh(reducedIntensityMatrix.*bp)
end

%Saving the aquired data
reducedIntensityMatrix=reducedIntensityMatrix .*placementGrid;
save('D:/Desktop/Technische natuurkunde/Jaar 3/Kwartiel ...
    4/BEP/Matlab-Script/Data/PlacementGrid.mat','placementGrid');
save('D:/Desktop/Technische natuurkunde/Jaar 3/Kwartiel ...
    4/BEP/Matlab-Script/Data/ReducedIntensity.mat','reducedIntensityMatrix');

w=[straal sigmaS sigmaA rho stepSizeCircle];
save('D:\Desktop\Technische natuurkunde/Jaar 3/Kwartiel ...
    4/BEP/Matlab-Script/Data/Constants.mat', 'w');

```

## D Matlab Mie Theory

The next three scripts calculate the Mie amplitude coefficients and the scattering and absorption cross sections. These scripts have mainly been made by Schepers<sup>[6]</sup>.

The first script takes as input the amount of discretization points for half of the Mie amplitude coefficients. Because these coefficients are symmetric only half have to be calculated. A stop criteria is determined for the summation of equations 80 and 81. The scattering coefficients  $a_n$  and  $b_n$  are calculated as are the coefficients  $\pi_n$  and  $\tau_n$ . With this  $S_1$ ,  $S_4$  and the cross sections are then calculated and some plots will be made depending on the input variable 'plot'.

```

function scattermatrix(thetaPoints,plot)
%input

```



```

theta=transpose(0:pi/thetaPoints:pi);
m=1.68;
a=5e-6;
r=a;
labda=532e-9;
k=2*pi/labda;
x=a*2*pi/labda;

%factor van bolgolf
bol=exp(1j*k*r)/(-1j*k*r);

%determine stopcriterion according to Bohren and Huffman
n=round(x + x^(1/3)+300);

%calculate scatter coefficients
[an, bn]=scattercoefficients(x,m,n);

[l, w] = size(theta);

%calculate angle dependent functions
[pin, taun]=pitau(theta,n);

%Calculate factors
fac=(2*(1:n)+1)./((1:n).*((1:n)+1));

%expand vectors as arrays to allow multiplication with angledependent
%functions
an= repmat(an',1,1);
bn= repmat(bn',1,1);
fac= repmat(fac',1,1);

%calculate full sum
S1n=fac.*(an.*pin+bn.*taun);
S2n=fac.*(bn.*pin+an.*taun);

S4=sum(S1n)';
S1=sum(S2n)';

%cross sections
Cscs=2*pi/(2*pi/532e-9)^2*sum((2*(1:n)+1)'.*(abs(an(:,1)).^2+abs(bn(:,1)).^2));
Cext=2*pi/(2*pi/532e-9)^2*sum((2*(1:n)+1)'.*real(an(:,1)+bn(:,1)));

theta=[theta' theta'+pi];
theta=theta';
theta(thetaPoints+1)=[];

S4=[S4' fliplr(S4')];
S4=S4';
S4=abs(S4).^2;
S4(thetaPoints+1)=[];

S1=[S1' fliplr(S1')];

```

```

S1=S1';
S1=(abs(S1).^2)./(k^2);
S1(thetaPoints+1)=[];

save('D:/Desktop/Technische natuurkunde/Jaar 3/Kwartiel ...
4/BEP/Matlab-Script/Data/S4.mat','S4');
save('D:/Desktop/Technische natuurkunde/Jaar 3/Kwartiel ...
4/BEP/Matlab-Script/Data/S1.mat','S1');
save('D:/Desktop/Technische natuurkunde/Jaar 3/Kwartiel ...
4/BEP/Matlab-Script/Data/Hoeken.mat','theta');

if(plot)
    figure, semilogy(theta*180/pi,S4./k^2)
    figure, semilogy(theta*180/pi,S1./k^2)
    figure, polar(theta, log(S4));
    figure, polar(theta, log(S1));
end

Cabs=Cext-Csca
Csca

```

The next script calculates the coefficients  $\pi_n$  and  $\tau_n$  as defined in equations 71 and 72.

```

function [pin, taun] = pitau(theta, n)
% %Angle dependent functions of theta. theta should be a horizontal
% %vector with small steps.

[l, w]=size(theta);

pin=zeros(n,l);
taun=zeros(n,l);

pin(1,:)=1;
pin(2,:)=3*cos(theta');

for i=3:n
    pin(i,:)=(2*i-1)/(i-1).*cos(theta').*pin(i-1,:)-i/(i-1).*pin(i-2,:);
end

taun(1,:)=cos(theta');
for i=2:n
    taun(i,:)=i.*cos(theta').*pin(i,:)-(i+1).*pin(i-1,:);
end

```

The next script calculates the coefficients  $a_n$  and  $b_n$  as defined in equations 70.

```

function [an, bn]= scattercoefficients(x,m,n)
%scatter coefficients an and bn as function of size parameter x and
%relative refractive index m.

%indices

```

```

nn=1:1:n;

% Differentiation step
h=0.0001;

%calculate spherical bessel function of the first kind with order n
jx=sqrt(pi./(2*x))*besselj(nn + 0.5, x);
jmx=sqrt(pi./(2*m*x))*besselj(nn + 0.5, m*x);

%calculate derivitive of xj
djx=((1+h)*x*sqrt(pi/(2*(1+h)* x))*besselj(nn + 0.5, (1+h)*x)-(1-h)*x* ...
      sqrt(pi/(2*(1-h)* x))*besselj(nn + 0.5, (1-h)*x))/((2*h)*x);
djmx=((1+h)*m*x*sqrt(pi/(2*(1+h)*m* x))*besselj(nn + 0.5, (1+h) *m*x)- ...
      (1-h)*m*x*sqrt(pi/(2*(1-h)*m* x))*besselj(nn + 0.5, ...
      (1-h)*m*x))/((2*h)*m*x);

%calculate spherical hankel function of the first kind with order n
hx=sqrt(pi/(2*x))*besselh(nn + 0.5, x);

%calculate derivitive of xh
dhx=((1+h)*x*sqrt(pi/(2*(1+h)*x))*besselh(nn + 0.5, (1+h)*x)-(1-h)*x* ...
      sqrt(pi/(2*(1-h)*x))*besselh(nn + 0.5, (1-h)*x))/((2*h)*x);

%compute scatter coefficients
an=(m^2*jmx.*djx-jx.*djmx)./(m^2*jmx.*dhx-hx.*djmx);
bn=(jmx.*djx-jx.*djmx)./(jmx.*dhx-hx.*djmx);

```

## References

- [1] The Nobel Prize in Physics 2014. cited June 25th 2015. <[http://www.nobelprize.org/nobel\\_prizes/physics/laureates/2014/](http://www.nobelprize.org/nobel_prizes/physics/laureates/2014/)>
- [2] C. F. Bohren, D. R. Huffman. (2007). Absorption and Scattering of Light by Small Particles. Weinheim. WILEY-VCH Verlag GmbH & Co. KGaA. ISBN 9783527618156. p. 82-129.
- [3] Akira Ishimaru. (1997). Wave propagation and scattering in random media. New York. IEEE Press and Oxford University Press. ISBN 0-7803-3409-4. p. 147-174.
- [4] David Ronald Kincaid, Elliott Ward Cheney (1996). Numerical Analysis: Mathematics of Scientific Computing. 2nd ed. University of Michigan. Brooks/Cole Publishing Company. ISBN 0534338925, 9780534338923.
- [5] J, Quant. (1996). T-MATRIX COMPUTATIONS OF LIGHT SCATTERING BY NONSPHERICAL PARTICLES: A REVIEW. Spectrosc. Radial. Transfer, Vol. 55, No. 5, pp. 535-515, 1996.
- [6] L.P.T. Schepers. (2015).
- [7] George C.-Y. Chan and WingTat Chan. (2001). Beer's Law Measurements Using Non-monochromatic Light Sources A Computer Simulation. J. Chem. Educ. Vol. 78 No. 9, p 1285, 2001.
- [8] Witold A. J. Kosmala. (2004). A friendly introduction to analysis, single and multi-variable. 2nd ed. New Jersey. Prentice Hall. ISBN 0-13-045796-5. p. 247, 354-355.
- [9] Carl Erik Frberg. (1985). Numerical mathematics: theory and computer applications. 3rd ed. University of Michigan. Benjamin/Cummings Pub. Co. ISBN 0805325301, 9780805325300.